uc3m | Universidad Carlos III de Madrid

Biomedical engineering degree

2017/2018

Bachelor thesis

Evaluation of the use of goat's milk-derived exosomes as theragnostic platform in oncology

---

Marina Cañadas Ortega

Supervisor

Beatriz Salinas Rodrígez

Lorena Cussó Mula

18 June 2018

ABSTRACT

Exosomes are biologically active nanovesicles from endosomal origin and lipid bilayer involved in cell communication, secreted by different types of cells and present in a wide variety of biological fluids. Due to their size, liposome-like characteristics and their strong relation with oncology, new applications for therapy and diagnosis are being explored in the field of medical imaging.

During this thesis, the isolation, characterization and functionalization with fluorescent dyes has been performed to examine the possibility of using goat's milk derived exosomes as theragnostic platform. With this purpose, the size, shape and charge of exosomes have been characterized, and the conjugation with two different fluorophores has proved to unalter their physicochemical properties. The biodistribution of functionalized exosomes, their toxicity and *in vitro* accumulation have been analyzed to evaluate that these nanovesicles can be used not only for diagnosis, but also for therapy and drug delivery in the future.

ACKNOWLEDGEMENT

En primer lugar, darle las gracias a Jorge, por estar siempre a mi lado apoyándome más que nadie, y sin el cual estos años hubieran sido mucho más grises. Gracias también a mi familia por hacer todo lo que estaba en su mano por darme un futuro mejor, tanto en el plano económico como en el emocional a pesar de la distancia. Gracias por haber creído siempre en mí. Gracias también a mis amigos de Madrid, especialmente a María, Moorina y Alberto por hacer de esta mi nueva casa, y gracias a mis amigas de Málaga (sois muchas y muy maravillosas como para nombraros a todas) por hacerme sentir que nunca me fui cada vez que vuelvo. Gracias a todos por haberme apoyado en cada aventura y plan que se me ha ocurrido y a la que os he arrastrado, y por darme fuerzas y ánimos cuando sentía que no podía más, ni con la tesis ni con la vida en general.

Finalmente, también me gustaría agradecer a todos aquellos que han dedicado su tiempo a formarme, desde profesores al personal de las distintas unidades del lab del Hospital Gregorio Marañón. En particular le doy las gracias a Bea y Lorena por guiarme en este proyecto, y a mis compañeros de la unidad de Sondas Moleculares (especialmente a Isa por enseñarme tanto y responder con paciencia todas y cada una de mis dudas). Gracias por confiar en mi capacidad y esfuerzo y por haberme ayudado a mejorar cada día más.

CONTENTS

LIST OF FIGURES

LIST OF TABLES

1. MOTIVATION AND OBJECTIVES

1.1. Motivation

Cancer is a generic term grouping a collection of different diseases with the common feature of the rapid growth of abnormal cells, which do not stop dividing and can spread to other organs or parts of the body [1]; it is an extremely complex disease for which many of their mechanisms of action remain unclear despite have been extensively studied over the years.

Roughly, one of every six deaths worldwide are caused by any type of cancer, being it the second leading cause of death. The number of deaths in the world in 2016 is estimated between 8.75 and 9.1 million by the Institute of Health Metrics and Evaluation (IHME) [2]; converting cancer in one of the diseases with higher incidence and human-life costs over the world population. For many types of cancer, the strongest chance of survivability and/or increased quality of patient's life during the treatment still resides in an early detection, before the tumour spreads to adjacent tissues or to distant organs through the blood or lymphatic system [3].

Different platforms have been developed for both early diagnosis and treatment of tumours, being many of them based on synthetic liposomes, which present serious disadvantages due to their chemical origin. The proposed work for this thesis is the use of natural liposome-like nanoparticles that would allow the non-invasive localization of both primary and metastatic tumours with a single screening, which would imply a time and cost-effective technique for early detection of cancer. Additionally, with further research it would be possible to use the aforementioned nanoparticles as drug carriers that will attach only the desired aberrant cells and their microenvironment without affecting the healthy tissue. For the present study, exosomes derived from goat milk have been used to determine their potential applications as a theragnostic tool applied in oncology.

1.2. Objectives

The main purpose of this Bachelor Thesis is the evaluation of caprine milk-derived exosomes as a new theragnostic platform in oncology.

To do so, several minor objectives have been stated, being (i) the optimization of extraction methods and purification methods by introducing changes to the most commonly

used techniques, (ii) the characterization of the resulting exosomes to ensure that the population of extracellular vesicles accurately corresponds to exosomes, (iii) the validation of the fluorescent labelling of exosomes for their use as molecular probes for cancer co-localization and (iv) the analysis of the effects of the exosomes both *in vivo* and *in vitro* (focusing mainly on toxicity, biodistribution and accumulation in tumours).

2. INTRODUCTION

2.1. Biological background

Exosomes are biological lipid bilayer-enclosed extracellular vesicles of endosomal origin, secreted by different tissues and cells under physiological and pathological conditions, being present in an extensive variety of body fluids (including serum, breast milk, saliva, tears, amniotic fluid or urine) [4] [5]. They are originated through the endocytic pathway by the fusion of multivesicular bodies with the plasma membrane [6], with functions related to the regulation of pathophysiological processes and cell communication, including immune responses, inflammation, tumour growth, infection and the modulation of concrete cellular activities [7] [4].

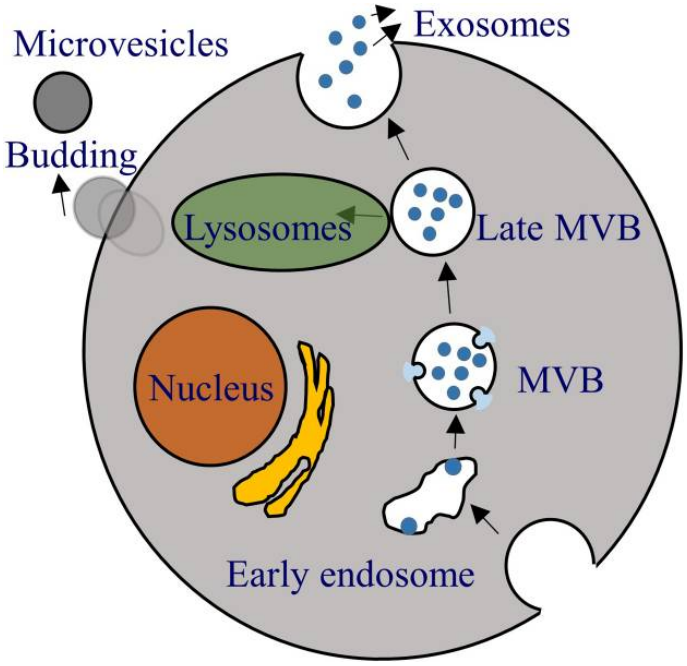

Fig. 1. Schematic representation of exosomes and microvesicles formation. Endocytic pathway involves the inward budding of endosomes into multivesicular bodies, which fuse with the membrane to release the exosomes [8].

It is important to differentiate between exosomes and microvesicles, since both are extracellular vesicles released by healthy cells to the extracellular space, with functions related with cell-cell signalling. Despite those similarities, exosomes and microvesicles are different populations within the extracellular vesicles with differentiated properties, sizes and characteristics as their lipid and protein composition, the shape of the membrane, the diffusion coefficient or their cargo content [9]. Thus, they are believed to have distinct roles in the regulation of a broad range of biological processes [10].

Exosomes are involved in intercellular communication and cell-cell signalling via their functionally active cargo, which contains miRNA, mRNA, DNA, lipids, metabolites and proteins related to transport, immunological responses and tumour progression [11]. Delving into the tumour-related functions of exosomes, these vesicles have shown determining relevance in oncology due to their active role in tumorigenesis, cancer progression, immune evasion and angiogenesis, since they have proved to be able of altering tumour microenvironments and to be related with the establishment of premetastatic niches and the remodelling of extracellular matrices [12] [13].

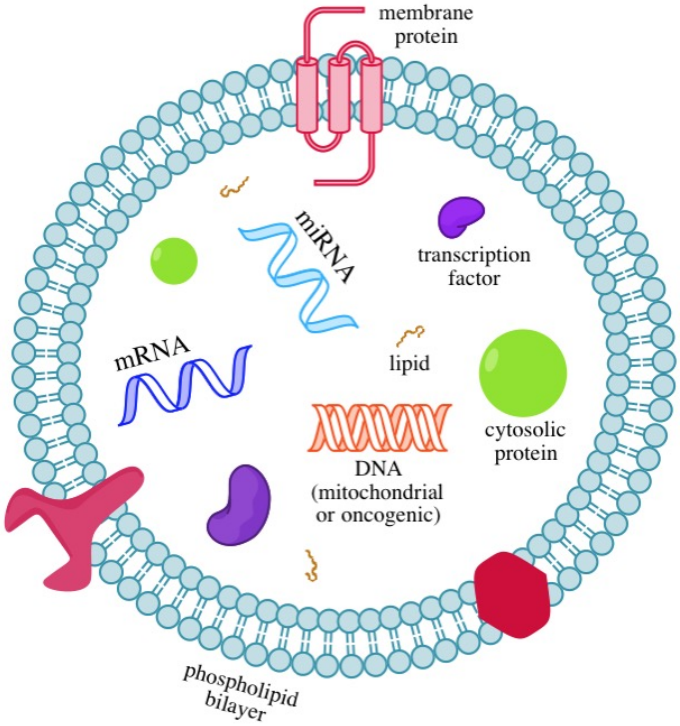

Fig. 2. Graphic representation of structure and content of exosomes[14].

Exosomes allow the exchange of information not only between neighbouring cancer cells but to communicate with different cell types at distant sites [15]. Recent studies have demonstrated that exosomes derived from cancer cell lines are able to promote metastasis of primary tumours [16], thus allowing the conditioning of the issue to allow colonization. Due to these properties related with tumour migration and pre-metastatic niches, the role of non-tumour derived exosomes is starting to be considered as well as their possible use as a non-toxic and biocompatible nanosized platform for drug delivery [12] [15].

2.2. Molecular imaging

Molecular imaging is a set of techniques that allow to visualize, characterize and measure biological processes at cellular level, favouring the study of pathways and disease mechanisms [17]. During last years, the impact of molecular imaging on the diagnosis and therapy of cancer has increased due to the possibility of combine morphologic, functional and metabolic techniques in an *in vivo* multimodal image [18]. Other advantages leveraged by this set of techniques are their capability of imaging alterations taking place at the molecular level, rather than the final effects of these changes and the high sensitivity and specificity of the techniques [19] [20]. Concretely applied to cancer, molecular imaging provides tumour location in the body as well as the visualization of the expression and activity of related molecules and biological processes that affect the tumoral behaviour [21].

Imaging applied to oncology is currently an integral part of diagnosis and therapy protocols, due to its capability of providing structural, metabolic and functional information, contributing enormously to the clinical decision-making, for example in the guidance of cancer treatments [22]. Additionally, it allows accessibility to the tumour without tissue damage, minimum invasion and real-time monitoring, which makes the techniques an important tool for early diagnosis [23].

2.2.1. Optical imaging

Optical imaging has emerged as an equally functional and non-invasive technique that enables real-time and high spatial resolution, presenting some advantages over the aforementioned techniques as their reduced side effects (since optical probes do not require ionizing radiation in comparison with the gold standard technique, nuclear imaging), financial costs (price of optical fluorescence cameras and probes is lower than those required for nuclear imaging) and their potential application in the identification of afflicted areas during interventions in guide surgery [26].

This technique takes advantages of visible light and the properties of photons to obtain insights into not only organs or tissues, but also cells and molecules; it is particularly useful for the visualization of soft tissues due to the varied absorption and scattering of light from different tissues. Additionally, the visualization of several properties or objects of interest can be done simultaneously due to the different spectrums provided by the available optical probes [27].

An important consideration of medical imaging probes is the requirement of an appro-

priate intensity of signal, sufficiently bright to be detected over the background noise and differentiable enough between structures of different tissues. In the development of new probes for biomedical applications, the use of liposomes (artificial phospholipid bilayer microvesicles) has experimented an increase in the last years due to their characteristics, among them standing the possibility of incorporating hydrophilic and hydrophobic fluorophores to their membrane structure [28]. As exosomes offer important advantages over liposomes [8], as it will be detailed in section 2.2.2, the use of labelled exosomes in optical imaging results of extreme interest.

2.2.2. Fluorescent probes

Fluorescence microscopy is an imaging technique based on the excitation of a fluorophore, that is, a molecule that can re-emit light upon light absorption, which, when illuminated with high energy light, emit light of a lower frequency allowing its detection on the microscope. This technique is of high importance since it can be used to detect and distinguish specific molecular components (called probes) inside the cells, which results of vital importance in the study of a broad amount of cellular processes [29].

Fluorescently conjugated probes are widely used to enable the visualization of events in cell death and assess cell viability. For the experimental procedures carried out in this thesis, two fluorophores were used: Cyanine and Sulfo-Cyanine 7.5 NHS Ester, which are near-infrared dyes used for the fluorescent labelling of exosomes with the intention to avoid the range of the light spectrum in which cellular components show autofluorescence [30].

Cyanine dyes are molecules containing polymethine bridges between two nitrogen atoms with a delocalized charge; NHS esters are the amine-reactive derivative of the aforementioned compounds. The differences between the two mentioned cyanine dyes reside in the presence of sulfo groups in the case of Sulfo-Cyanine, rendering the dye hydrosoluble instead of requiring organic co-solvent as Dimethyl Sulfoxide (DMSO) and affecting the molecular weight of the probe. Additionally, sulfonated cyanines are less prone to aggregation due to the charged sulfonate groups. The differences in the spectral properties are minimum, having both maximum excitation at 750 nm and emission and 773 nm [31].

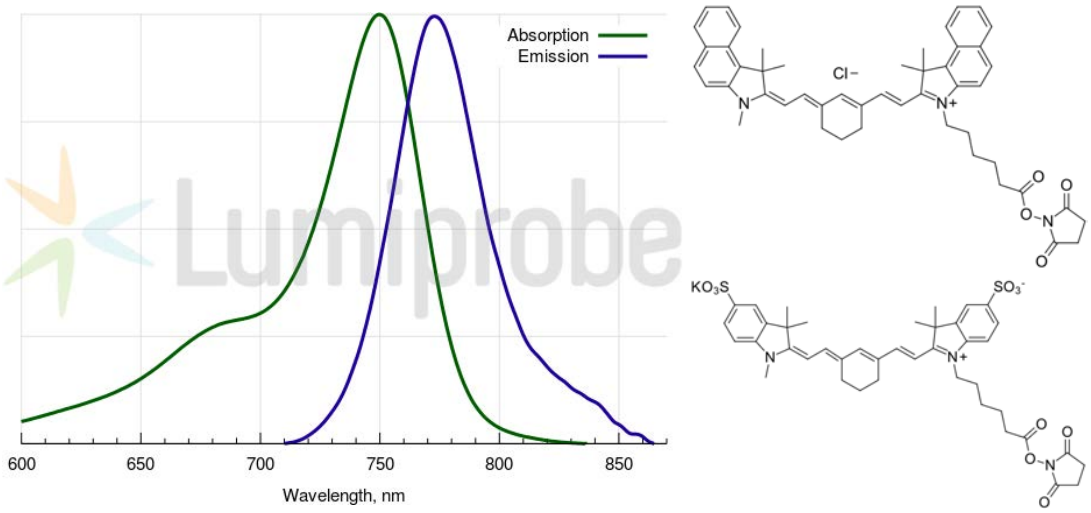

Fig. 3. Absorption and emission spectra of Sulfo-Cyanine 7.5 NHS ester (left). Molecular structures of Cyanine (top right) and Sulfo-Cyanine (bottom right) [31].

2.3. Technological relevance

Cancer is one of the deadliest groups of illnesses worldwide, and increasing the effectiveness of treatments with early detection, together with the finding of non-invasive biomarkers for abnormal tumour cells result of enormous importance. Additionally, this detection methods suppose a significative contribution to currently used techniques as fine needle aspiration, which obtain samples "blindly" from tissues, relying to locate and access the tumour at first attempt. Using exosomes as markers for localization, tumours can be non-invasively situated, improving sample collection and treatment localization, preventing in this way unnecessary manipulation of healthy surrounding tissues [32].

Advances in the development of specific imaging techniques carried out during the last years have found obstacles regarding the clinical applications, mainly limited by toxicity of the probes, host immune responses or difficulties in their large-scale production in a cost-effective way. The use of exosomes as platform for medical imaging in oncology would overcome most of these drawbacks. Due to their lipidic layer and liposome-like structure and behaviour, thoroughly described in literature [28] [33] [34], exosome exploitation as drug carrier offers all the advantages considered for liposomes, without the drawbacks of these synthetic nanoparticles. Thus, these naturally derived nanoparticles have a strong potential as chemotherapeutic agent and drug delivery vehicle, being a possible solution for the limitations of synthetic nanoparticles. This is due to several advantages that include the following:

- Their tolerance and non-toxicity within the own body and when injected in foreign species. Concretely, investigations have showed that bovine milk exosomes are cross-species tolerant, causing no immunological or inflammatory effects [15] [35].

- The presence of an active cargo within the exosome that can be altered to use exosomes as drug carriers [15].
- Their ability to be internalized by cells [36].
- The possibility of attachment of ligands to increase the targetability and direct the drug delivery [8].

Despite the advantages exhibited by exosomes over other synthetic liposome-like nanoparticles and over other natural particles used for the same purpose - as mesenchymal cells [37] [38] -, different sources of exosomes are currently known. Between those, milk exosomes were used instead of human-derived ones for two main reasons: there is a need for safe, scalable and profitable method of production of exosomes, and the security that no adverse effects are caused [15].

- On the contrary to human exosomes, goat's milk is readily available and easy to obtain, allowing an easy to overcome step through their high production and commercialization; also, they don't entail biocompatibility problems as caprine and bovine milk have been ingested by human beings for millenniums, ensuring at first glance that no toxic effects are caused.
- The main advantage of milk-derived exosomes compared to other types of exosomes, as tumoral ones, is their absence in participation of pre-oncologic processes, as it was demonstrated that oncogenic cells produce miRNA that induces tumorigenesis and thus, further tumour progression and metastasis [39].

With respect to the use of milk resulting from goats instead of cows, it is due to the lower amount of fat present in caprine milk, which leads to a reduced number of purification steps, which necessarily increases the preservation of the exosome. This causes the extraction process to be easier and less time-consuming (which is one of the main drawbacks of the isolation technique) [40] [41].

Additional advantages of using exosomes over any other type of synthetic nanoparticles is the possibility of conjugation with other biological molecules or dyes without the alteration of their membrane or properties due to the presence of lipids and biomolecules in the surface. This allows the functionalization with fluorescent probes, which permit non-invasive tracking *in vivo* using molecular imaging.

The last important factor that must be taking into account when considering the use of exosomes as a new theragnostic platform for oncology is that, as liposome-like synthetic particles, exosomes take advantage of the Enhanced Permeability and Retention Effect (EPR), which enhances their accumulation in tumours. Thanks to this effect, nanoparticles and other small particles have a tendency to accumulate in tumour tissues due to

the angiogenesis produced by Vascular Endothelial Growth Factors (VEGF). These new vessels that nurture solid tumours are characteristically leaky, with reduced lymphatic drainage; this causes the nanoparticles (which are generally stable in circulation when they are sufficiently small to avoid the detection by the reticuloendothelial system but at the same time not small enough to be excreted through the kidney) to leak through the permeable tumour vasculature and to be retained there due to the poor lymphatic drainage [42].

2.4. State of the art

Exosomes have been a hot topic during the last years due to their role in numerous processes; particularly related to oncology, they have been widely used as tumour biomarkers. Moreover, their size in the range of nanometres, natural origin and liposome-like structure suggest their use as nanocarriers for both diagnostic and therapeutic applications [8].

Because of this, multiple studies have been performed with exosomes. Most of them focus on their role in the modulation of the immunological response [4] [5], studying human-derived vesicles; others try to determine their internalization method, their secretion pathway or their cargo content. Some researches focus on the applications of milk-derived exosomes as drug carriers [6] [15] while further ones attempt to detect the cancerous exosomes from the human liquids where they are found [43] in a novel technique known as exosome-based liquid biopsy. Furthermore, it has been demonstrated that the exosomal cargo varies between healthy and tumour cells [35], allowing the detection of the presence of a tumour by analysing the cargo content of the exosomes [43]. This differential expression is linked to unbalanced homeostasis and constitutes a reflection of the metabolic state of the cells of origin by presenting concrete specific surface proteins and the parental RNA and protein profiles [39]. These investigations confirm that exosomal nucleic acids can be utilized to find genetic signatures in patients with cancer.

As it can be seen, most of the research currently performed focus in the alteration or identification of the cargo for drug delivery or specific cancer detection. However, the intended approach of this work differs in the diagnosis method: instead of collecting samples related with the suspected origin of the tumour (liquid biopsy) and using the exosome cargo (either miRNA, proteins or other content) as biomarkers, labelled exosomes would be used as molecular markers and, by molecular imaging techniques, the tumour would be detected with independence of its origin. With this spatial information, further analysis could be performed, as the collection of the body fluid or the fine aspiration needle technique for confirmation of the type of tumour.

Although the study of the use of exosomes has suffered a dramatic increase during last years, little work has been found related with the use of the exosome itself as a molecular probe in the biomedical imaging field [15] [44].

3. MATERIALS AND METHODS

For the evaluation of goat's milk derived exosomes as theragnostic paltform in oncology, the experiments were focused in several areas: first, in the development of an optimized protocol for the extraction of pure exosomes and their characterization; then, in the improvement of a conjugation method to allow the detection and tracking of exosomes with optical imaging, and finally, in the evaluation of the effects of exosomes in vitro. To do so, their toxicity and uptake were assessed in different types of cells. Additionally, the conjugation technique was evaluated to test its robustness not only with milk exosomes but with exosomes derived from cancer cells; for this validation, cancer exosomes were isolated, characterized and conjugated.

The different sections detail the techniques used for the extraction and purification of the exosomes to obtain the most genuine extract possible, their characterization to claim that the expected nanovesicles are obtained, their conjugation to allow their use in molecular imaging, and the studies of uptake and toxicity in tumours and organs.

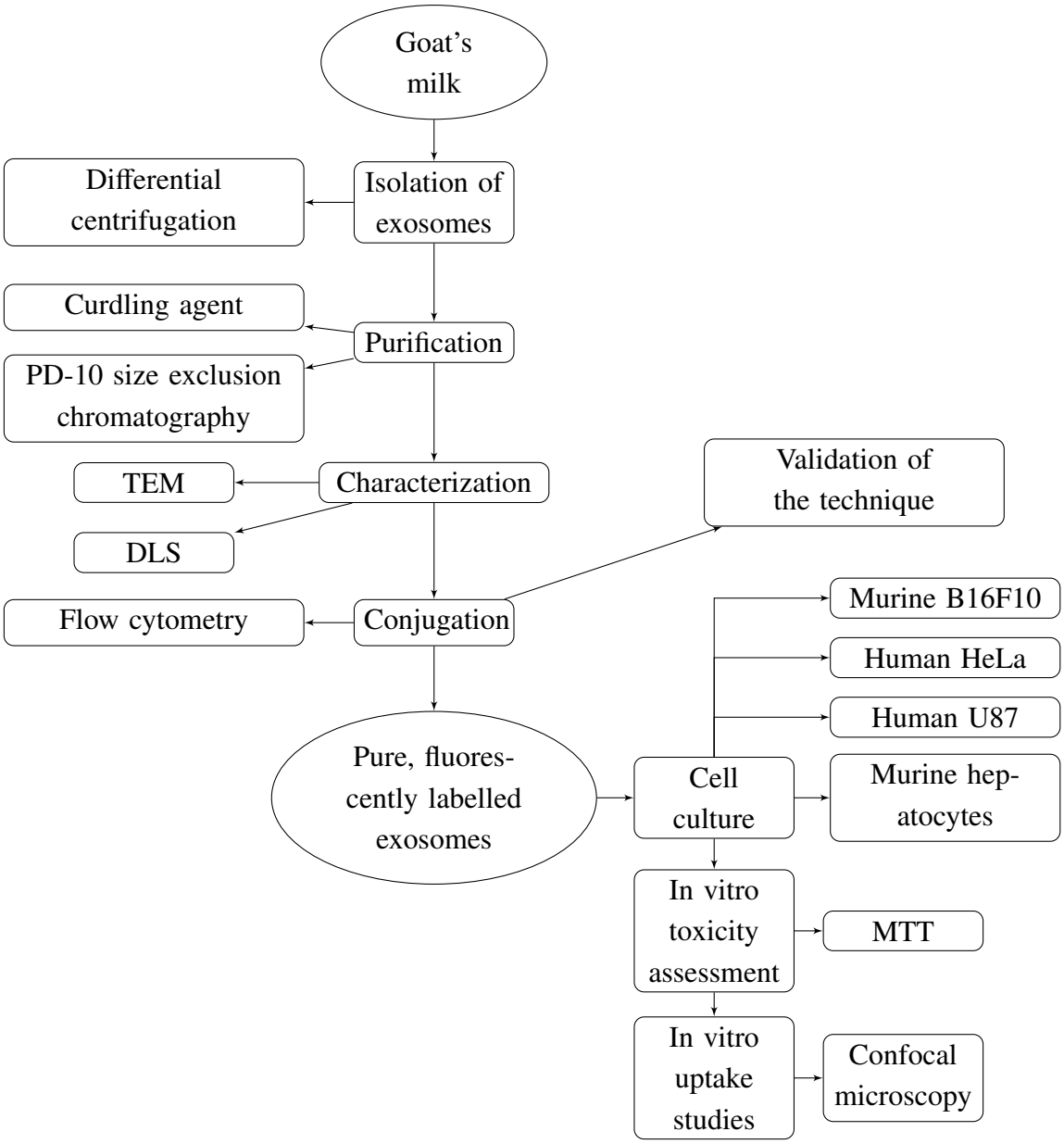

Fig. 4. Flowchart of the different experiments carried out to complete the stablished objectives.

3.1. Milk collection

One litre of commercial skimmed pasteurised goat's milk 'Cantero de Letur' was acquired at the market and stored at 4^{o}C for exosome isolation within the next days.

One litre of fresh whole unpasteurised goat's milk (unknown week of lactation) collected from a dairy herd located on the outskirts of Madrid. Milk was kept refrigerated until its arrival and then, aliquoted (40 ml) and stored at -20^{o}C until its use.

3.2. Isolation and purification of milk exosomes

Isolation of exosomes derived from goat's milk by means of differential centrifugation and ultracentrifugation was performed based on protocols from Munagala, Radha et al. [15] and Vaswani, Kanchan et al. [45] combined with curdling agent used for further protein precipitation and increased number of low speed and ultracentrifugations (>50,000 x g) [46]; an additional purification step with PD-10 desalting columns was introduced, resulting in the optimized protocol presented in Fig. 5.

Protocol#	Number of low speed centrifugations	Number of ultra-centrifugations	Curdling agent	Filtration
Munagala et al	1	2	No, but cheese colth used	0.22 μm
Vaswani et al	2	2	No	qEV column
Optimized protocol	4	5	Yes	PD-10 columns

Table 1. Comparison of different methods for isolation of milk exosomes

Briefly, milk aliquots (30 ml) were centrifuged at 5,000 × g in 50 ml polycarbonate tubes with cap (Beckman Coulter, Brea, California) using a JA 30.50 Ti fixed 34° angle rotor and Avanti J-301 centrifuge (Beckman Coulter) at 4°C for 10 minutes to eliminate fat globules and the main layer of fat. The supernatant is collected and a 0.5% with respect to the original volume of the sample of curdling agent is added; the polycarbonate tubes containing the mixture are incubated during 20 minutes in a static system (a water bath is used) and then centrifuged at 5,000 x g for 10 minutes at 4°C with the aforementioned centrifuge in order to remove rests of fat and curdling agent. The supernatant is collected and centrifuged at 13,000 × g, 4°C for 30 minutes to separate exosomes from microvesicles. This procedure is then repeated at 35,000 × g for 35 minutes to precipitate casein and cell debris and at 100,000 × g at 4°C for 60 min to precipitate exosomes. This supernatant is discarded and the exosome pellet obtained is washed and resuspended with PBS (Sigma-Aldrich, St. Louis, MO) to give homogeneous suspension. The resuspended exosomes in PBS are centrifuged at 100,000 × g at 4°C for 90 minutes, the supernatant discarded and the pellet of exosomes resuspended in PBS; this procedure is repeated three times to ensure the precipitation of exosomes. After the third ultracentrifugation, the pellet of exosomes is resuspended and pooled in PBS and filtered using a PD-10 desalting column (Sigma-Aldrich) with bed size of 14.5 mm × 50 mm, which allows the pass of particles of size ranging between 85 and 260 μm. Eluted fractions 2 and 3 are collected while the rest (1, 4, 5 and 6) are discarded. The exosomes are then pooled in PBS and centrifuged at 100,000 × g for 90 minutes at 4°C to cause precipitation; the supernatant is discarded and the pellet is resuspended to give homogeneous suspension. The total protein content of exosomes is determined and stored in aliquots at -20°C until use.

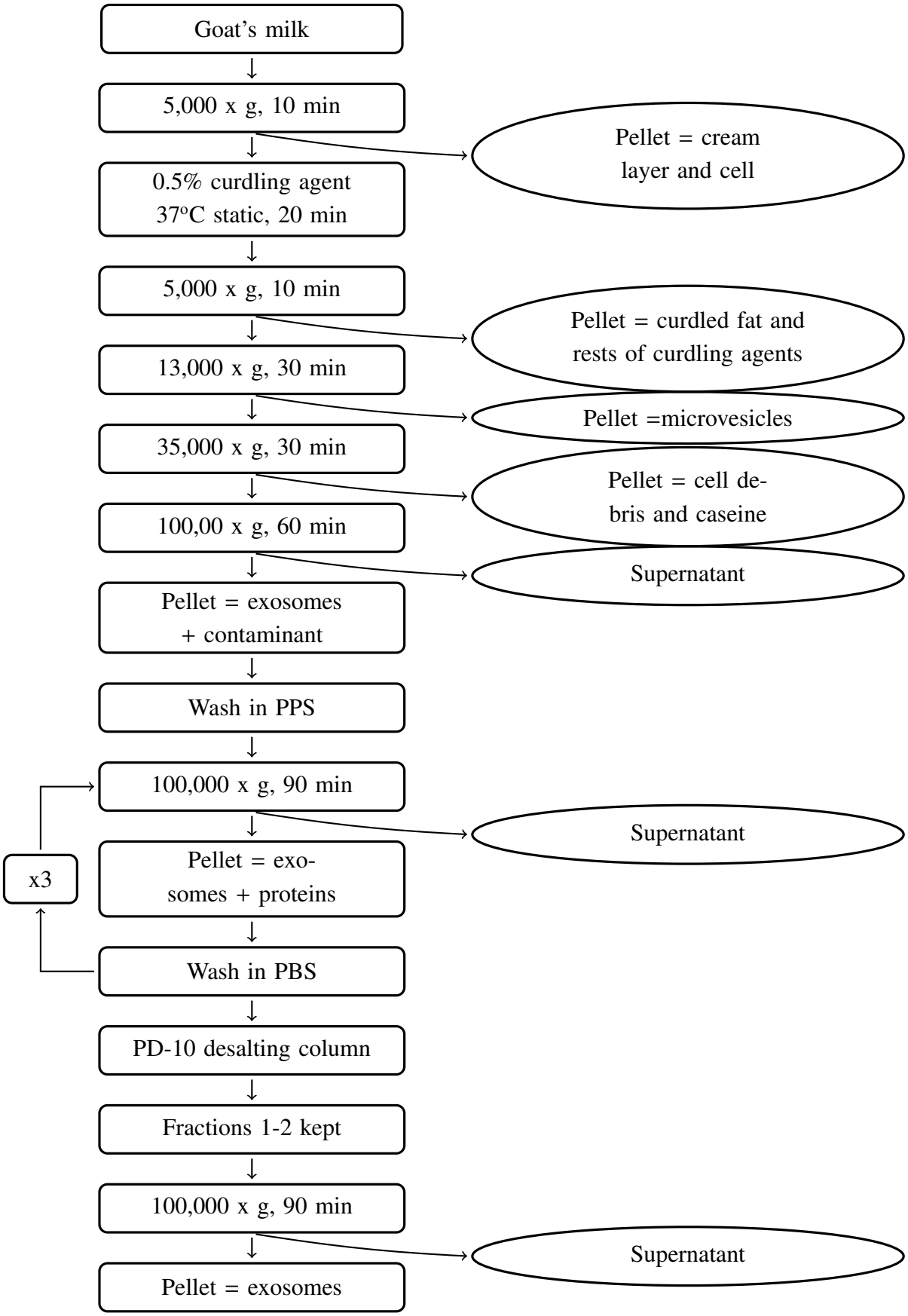

Fig. 5. Flowchart of the optimized protocol developed for the isolation and purification of goat's milk derived exosomes.

3.3. Protein determination

An estimation of protein content of aliquot of isolated exosomes is determined by comparing the protein concentration from the sample with two standard calibration curves made with known concentrations of albumin from bovine serum (lyophilized powder, $\geq$ 98%, Sigma-Aldrich). EZBlue gel staining reagent (Sigma-Aldrich) was used to allow the measurement of their respective absorbances at 595 nm and the mathematical calculation of the concentrations was performed with a MATLAB code of own development.

3.4. Transmission Electron Microscopy

Exosomes were filtered using 0.45 μm Millex-HP syringe filter (Merck KGaA, Darmstadt, Germany) and diluted 1:100 in PBS; then transported in ice to the National Centre of Electronic Microscopy in the Complutense University of Madrid. The negative staining was performed by a technician according to procedure from literature [47]. Briefly, samples were placed on coated copper grids, then washed with ultrapure water and negatively stained. Transmission electron microscopy (TEM) images were acquired using a JEOL 1010 TEM (JEOL USA, Inc) by the technician.

3.5. Dynamic Light Scattering

Exosomes were filtered as described previously and transported to the Spanish National Center of Cardiovascular Research of Madrid. The size distribution and zeta potential of the isolated exosomes was obtained using a Zetasizer Nano ZS (Malvern Instruments) and disposable cuvettes DTS0012 (Sigma-Aldrich) according to manufacturer's instructions. All samples were evaluated in 3 replicates.

3.6. Flow Cytometry

The Gallios 10 colors, 3 lasers Flow Cytometer (Beckman Coulter) of the Foundation for the Biomedical Investigation of the Gregorio Marañón Hospital was used for flow cytometric analysis of blank and fluorescently labelled exosomes. Samples were diluted 1:100 in PBS to avoid saturation and loaded in round-bottom polystyrene tubes for the analysis with the cytometer [48]. For the data acquisition and analysis (definition of gates and assay of the fluorescence), Kaluza Acquisition Software was used; for all analyses, light-scattering detection was performed in log mode. The maximum number of events and the event rate was not restricted.

3.7. Conjugation of milk exosomes with fluorophores for molecular imaging

Goat's milk derived exosomes were conjugated with Sulfo-Cyanine 7.5 NHS ester and Cyanine 7.5 NHS ester according to manufacturer's instructions; the procedure is the same for both dyes. Briefly, exosomes are brought with PBS to a final volume of 100 μl; pH is measured with pH test strips (Sigma-Aldrich) and raised up to 8.5 using 0.1 M sodium bicarbonate (Sigma-Aldrich). A proportion 1/10 of stock Sulfo-Cyanine 7.5 NHS ester (scy7.5) dissolved in ultrapure water with a concentration of 16.9 mM is added to the exosomes. The mixture is kept at 4°C in a shaker at 750 rpm in the dark for 4 hours.

The conjugate is purified using Exosome Spin Columns MW 3000 (Thermofisher Scientific, Holsville, NY) according to manufacturer's indications: column is hydrated with PBS and allowed to achieve gelation, then the excess of PBS is removed by centrifugation and the sample is charged; the excess of dye is cleared away with further centrifugation.

3.8. *In vivo* biodistribution in healthy animal

Two healthy mice (n = 1 per group) were used to analyse the biodistribution of exosomes administered via intravenous injection of exosomes conjugated with fluorophore and the NIR fluorescent dye itself. The procedure was carried out by the Molecular Probes group of the Foundation for the Biomedical Investigation of the Gregorio Marañón Hospital without my contribution, although the results obtained were significant for my posterior studies.

3.9. Cell culture

Mouse melanoma (B16F10), human adenocarcinoma (HeLa) and glioblastoma (U87) and mouse primary hepatocytes were ceded by the Cell Culture Unit of the Gregorio Marañón Hospital. All cell lines were supplemented with 10% heat-inactivated foetal bovine serum (Gibco, Life Technologies USA) and 1% glutamine (Thermofisher Scientific). FBS had previously been centrifuged at 100,000 × g for 3 hours and filtered with a 0.22 μm filter to remove bovine exosomes that could interfere with the studies. The B16F10 cells were grown in RMPI, the HeLa, U87 and hepatocytes were in DMEM (Lonza/Clonetics Corporation, San Diego, CA). All cell lines were cultivated at 37°C and 5% CO_2 in a humidified chamber.

Primary hepatocytes were isolated by the hepatogastric lab of the Foundation for the Biomedical Investigation of the Gregorio Marañón Hospital, headed by Dr. Javier Vaquero. Cells were obtained by smashing and filtering the liver of euthanized mice to disregard the tissue. Differential centrifugation using Percoll solution (Sigma-Aldrich) was performed to obtain isolated hepatocytes, which were sow in attachment media in culture plaques with their bottom previously covered with a 1:1000 solution of collagen type I (Sigma-Aldrich). Attachment media is made with DMEM, F12 (Thermofisher Scientific), glutamine, HEPES (Thermofisher Scientific), glucose, inactive FBS, BSA and antibiotic. Media was changed every day or before the addition of exosomes -depending on the requirements of the experiment- using regular DMEM without exosomes.

3.10. Isolation of exosomes derivative from cancer cells

The isolation was performed using a simplified differential centrifugation protocol with no purification steps described in literature [52].

The cellular medium where the different cancer cells (B16F10, HeLa, U87) were cultured was aliquoted and stored at -20^{o}C until the extraction of exosomes. The same centrifuge and tubes than the described in section 3.2 from methodology were used. Briefly, 60 ml of each type of cell medium was centrifuged at 300 x g for 10 minutes to eliminate cells. The supernatant was then collected a centrifuged at 2,000 x g for 10 minutes to eliminate dead cells, subsequently at 10,000 x g for 30 minutes to get rid of cell debris and finally at 100,000 x g for 70 minutes to precipitate the exosomes. The supernatant was discarded and the pellet of exosomes was washed and resuspended in PBS, then centrifuged at 100,000 x g for 70 minutes and resuspended in PBS to increase the purity of the isolated exosomes.

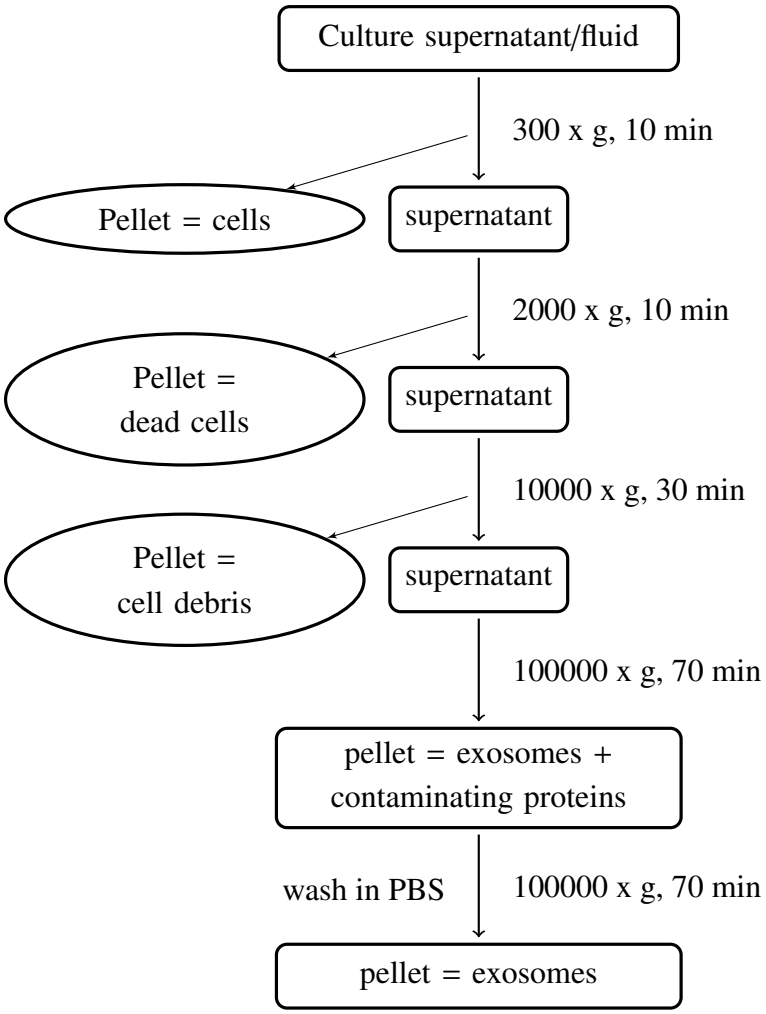

Fig. 6. Flowchart summarizing the process of isolation of exosomes derived from tumoral cells from Thery et al. [52]

3.11. Characterization and conjugation of cancer cells exosomes

Exosomes derived from cancer cells were conjugated applying the same protocol used for the functionalization of milk exosomes (section 3.7) and characterized using the aforementioned techniques employed for the characterization of goat's milk derived exosomes (protein determination (3.3), TEM (3.4), DLS (3.5) and flow cytometry (3.6)).

3.12. *In vitro* toxicity assessment

Potential short-term toxicity of exosomes was tested *in vitro* for all previously mentioned cell lines using MTT assay. Cells were first cultured for 24 hours in 96-well plates. To improve the attachment of cells to the bottom of the culture plaques (Costar, Sigma-Aldrich), they were covered with dissolution 1:1000 of collagen type I (Sigma-Aldrich)

up to a 5% of the maximum volume of the well; then sterilized in ultraviolet light for an hour at room temperature before seeding. Tumor cells previously grown in flasks (Sigma-Aldrich) with less than three passages were lifted and quantified in a Neu Bauer chamber (Sigma-Aldrich) according to the product instructions. Hepatocytes were obtained as described in section 3.9; the counting was performed following the same procedure as for tumor cells. Roughly 5,000 cells, either cancer or liver cells, were seeded in 200 μl of their corresponding cell culture media per well, and incubated overnight at 37^{o}C.

Doses of different concentrations, usually of subsequent orders of magnitude (50, 5, 0.5, 0.05 μg/ml) were added and incubated for either 24 or 48 hours before the MTT assay. To assess the toxicity, 1/10 of Thiazolyl Blue Tetrazolium Bromide (powder, 98%, Sigma-Aldrich) with concentration 5 mg/ml is added per well and incubated over 3 hours at 37^{o}C. After that period, the whole content of the wells is removed and 100 μl of Dimethyl Sulfoxide (Sigma-Aldrich) is added per well to dissolve the formazan crystals formed. Incubation at room temperature in shaker for half an hour is performed to improve the dissolution of these crystals. Then, absorbance is measured at 595 nm.

3.13. *In vitro* uptake studies

The uptake of exosomes by cancer cells (B16F10, HeLa and U87) was assessed with confocal microscopy as described in next section. For sample preparations, culture plaques were prepared by introducing one cover slip glass per well and covering 1/7 of the well volume with dissolution 1:1000 of collagen type I solution, then sterilized in ultraviolet light for an hour at room temperature. Collagen removed before seeding of 20,000 tumour-derived cells from previously grown flasks with less than three passages in 500 μl of their corresponding cell culture media per well. Cells were incubated overnight at 37^{o}C before the former study.

Different doses of sulfo-cyanine conjugated exosomes (5 and 0.5 μg/ml) were added at separated times (30 min, 1, 2, 4 and 24 hours) in order to allow the fixation of all cells at the same time point to avoid variability between samples. In this way, all cells were cultivated for the same period of time, being the differences in viability and uptake attributable to the effect of exosomes and not to the different times passed between the seeding and the sample. For example, if fixation is to be performed at 1 PM of day 2:

- 24 h dose will be added at 1 PM of day 1.
- 4 h dose will be added at 9 AM of day 2.
- 2 h dose will be added at 11 AM of day 2.
- 1 h dose will be added at 12 PM of day 2.
- 30 min dose will be added at 12:30 PM of day 2.

3.14. Confocal microscopy

Fixation of samples from uptake studies was performed by adding the same amount of formaldehyde 4% (Sigma-Aldrich) as culture media was in the wells, and incubating at room temperature for 5 minutes. After that time, the content of the wells was carefully removed with a pipette to avoid the aspiration of cells and 500 μl of PBS are added.

For the assembly of microscope slides, 200 μl of 4,6-diamidino-2-phenylindole 1:5000 (Sigma-Aldrich) were added per well and incubated 5 minutes at room temperature. Slip glasses were lifted from the wells using pliers, washed in ultrapure water and placed into covers using DAKO mounting media (Agilent, Palo Alto, CA). All quantifications were performed in a blinded way. Image acquisition was carried out using the glycerol ACS APO 20x NA0.60 immersion objective of a confocal fluorescence microscope (SPE, Leica-Microsystems). To allow visualization of the near-infrared dye, excitation was carried out at 647 nm.

Fiji was used for visualization and manipulation of the obtained images. Contrast and brightness were adjusted for the merged images between channels. A small circular region of interest (ROI) similar to the size of an U87 cell nucleus (13 $\times$ 14 pixels) was defined and used to compare the intensity of sulfo-cyanine in the near-infrared channel at the different time points of uptake. These intensities were normalized with respect to the background [49].

4. RESULTS

4.1. Isolation and purification of milk exosomes

Extensive amounts of proteins were satisfactorily removed with the developed protocol, forming a layer of fat separated from the supernatant in the centrifuge tubes. The use of curdling agent further improves the precipitation of fat, yielding exosomes with reduced protein contamination when passed through the size-exclusion chromatography. The protein content of the fractions obtained from the PD-10 desalting columns was obtained in order to optimize the recovery of exosomes and the elimination of the maximum amount of contaminant proteins.

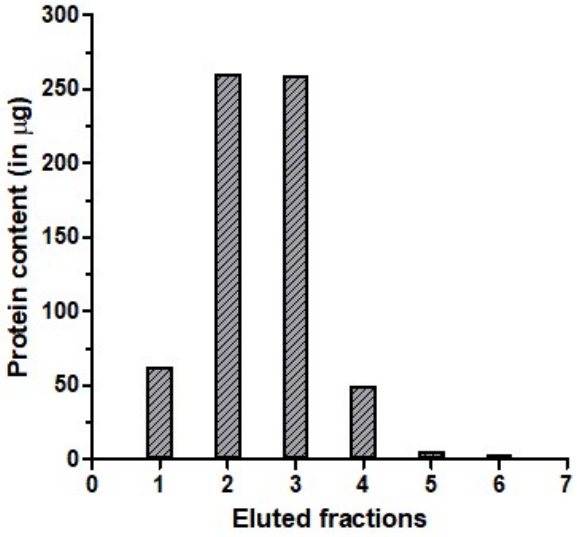

Fig. 7. Protein content of the PD-10 fractions. Exosomes isolated from 60 ml of commercial milk were passed through the desalting column and eluted with PBS in 7 fractions. Proteins were only noticeably present in fractions 1-4.

Exosomes start eluting in fraction 1, coeluting with small proteins, and continue in fractions 2 and 3 with a high yield of exosomes. Fractions 4 and 5 contained only contaminant proteins, being discarded. The bulk of proteins elutes in fractions 2 and 3, being their protein content 5 times higher than the content of fractions 1 and 4, as can be seen in Fig. 7; this could be observed at naked eye since the turbidity of the fractions was maximum for fractions 2 and 3, and almost unnoticeable in the rest. The fractions were analysed with TEM (Fig. 8), not as a qualitative characterization, but to check whether the increased presence of exosomes in the fractions correlates with the protein content analysis.

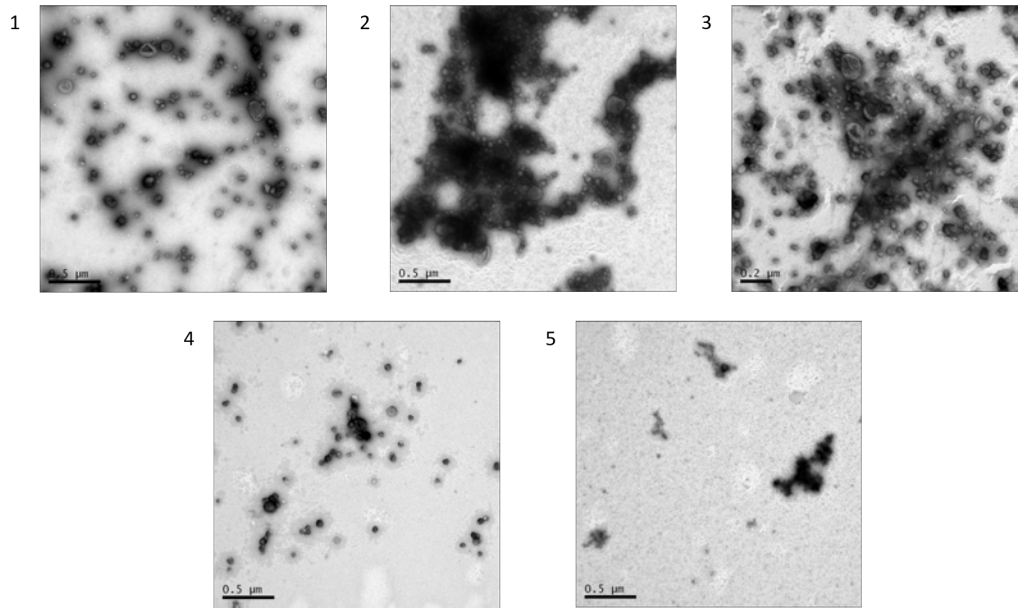

Fig. 8. Transmission electron microscopy comparing the eluted fractions from the PD-10 column. Images 1, 2, 4 and 5 were visualized using a magnification of 40,000 x; image 3 has a magnification of 60,000 x.

When selecting fractions 2 and 3, the amount of contaminant proteins is reduced and the exosomes yield high purity, being easily identifiable. The result of analysing the protein content of the purified exosomes (when the appropriate fractions are selected) after the optimized protocol is approximately of 199.3 ± 8.4 μg per 30 ml of commercial pasteurised milk (n = 4).

Additionally, the optimized protocol was used to obtain exosomes from different types of milk in order to check the robustness of the method. Concretely, the protein content per 30 ml of fresh unpasteurised milk was of 501.8 ± 24.3 μg (n=4). Higher amount of obtained proteins (more than twice) and variability is observed for the unpasteurised milk in comparison with the pasteurised milk.

4.2. Characterization of exosomes

The physicochemical properties of the obtained nanoparticles are examined and characterized according to a variety of techniques to determine that the product obtained actually corresponds to exosomes:

4.2.1. Transmission Electron Microscopy

Morphology and size were visually inspected, as well as the purity with respect to proteins of the sample. The isolated vesicles are visually identified as exosomes (Fig. 9 panel

a), having the expected cup-shape, size and intact morphology according to literature.

The shape and morphology of fresh unpasteurised milk-derived exosomes was also characterized with TEM to visualize the differences in protein contamination (Fig. 9 panel b). Observed abundance within the field of view is higher in unpasteurised milk, together with a higher presence of protein contamination in comparison with commercial milk. Additionally, differences in size can be observed between the exosomes derived from commercial pasteurised and from natural untreated milk, being the former smaller than the latter.

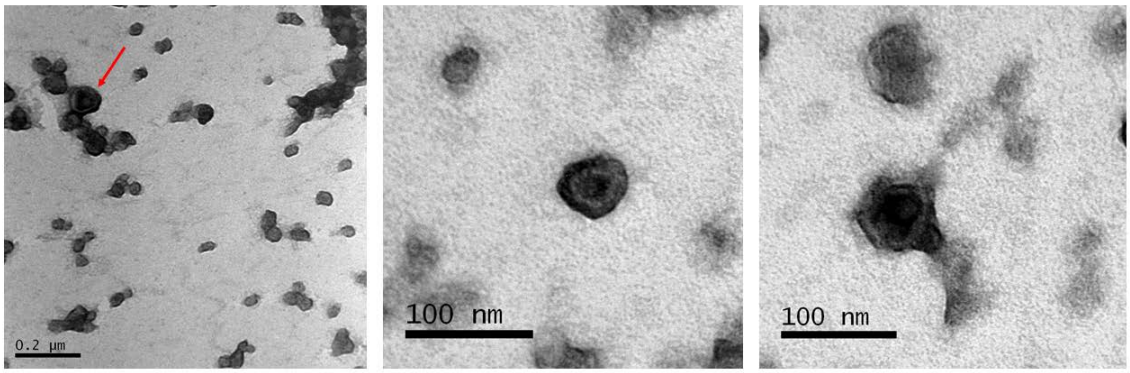

(a)

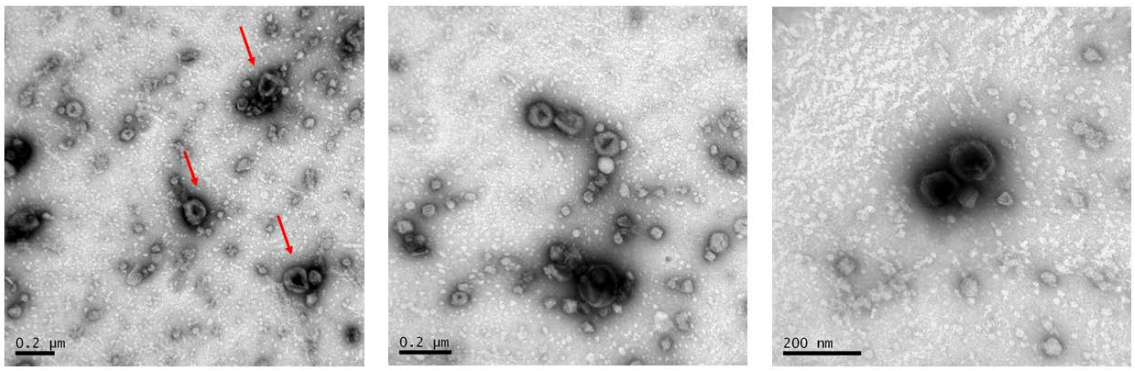

(b)

Fig. 9. Transmission electron microscopic observation of morphology of isolated vesicles from commercial pasteurised (a) and unpasteurised (b) goat's milk with the optimized protocol. Top left image was acquired with 80,000 x magnification, while top center and right images have 200,000 x magnification. For bottom images, from left to right they were acquired with 60,000 x, 80,000 x and 120,000 x magnification, respectively.

4.2.2. Dynamic Light Scattering

The hydrodynamic size distribution of the exosome populations was determined using Dynamic Light Scattering (Fig. 10). For commercial pasteurised milk, the size distribution presents a narrow shape, obtaining a mean value of 135.32 ± 9.12 nm (n = 3), while for the untreated milk the shape is broader and the typical size of exosomes is 221.85 ±

26.50 nm (n = 3). Additionally, the Z potential of pasteurised milk was measured, giving a value of -12.57 ± 0.58 mV.

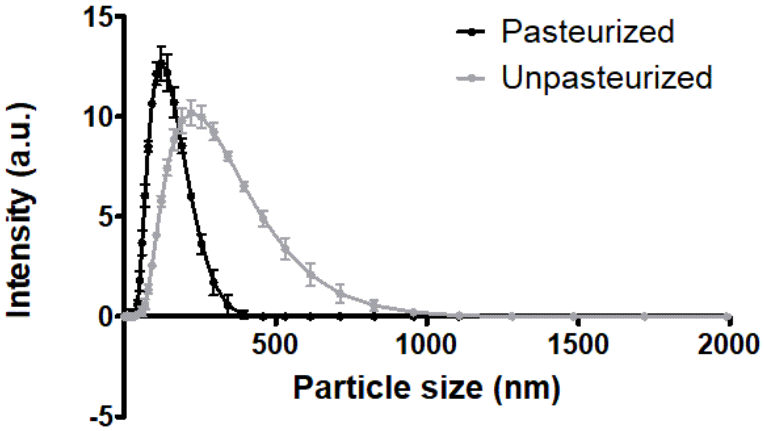

Fig. 10. Hydrodynamic size distribution of commercial and natural exosomes using Zetasizer Nano ZS.

4.3. Conjugation of milk exosomes with fluorophores for molecular imaging

Exosomes derived from commercial milk were destroyed when conjugated with regular Cyanine 7.5 NHS ester dissolved in DMSO; with the addition of the dye to the blank exosomes, difficulties in homogenisation were found, and the formation of an unexpected solid precipitate was noticed (Fig. 11 left image). After the reaction, it was noticeable the apparition of two differentiated phases, one coloured and with a solid precipitate in the bottom, and a transparent phase in the top. When purified with Exosome Spin Columns, all the dye was retained in the top of the column, resulting in a low conjugation yield as the typical green product was barely detectable (Fig. 11 centre and right images, right samples respectively).

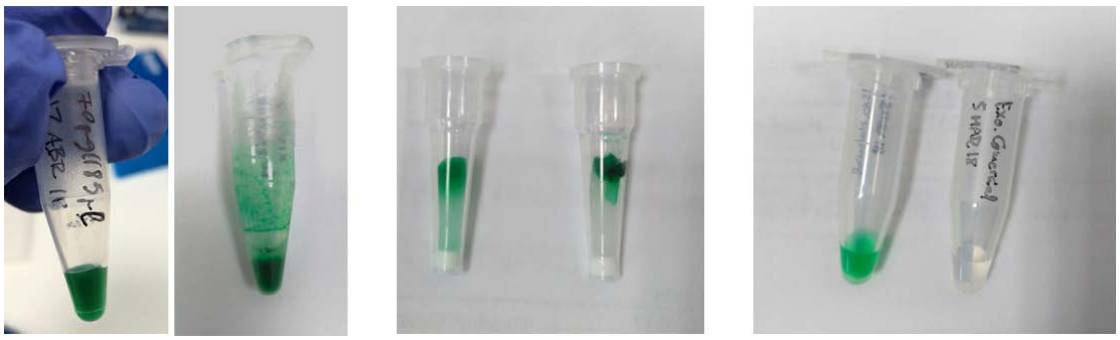

Fig. 11. Procedure: homogenisation of dyes (left images) with commercial milk-derived exosomes, purification columns after the loading of the samples (centre) and final product (right). In each image, the Sulfo-Cyanine is presented at the left, while the samples conjugated with Cyanine is at the right.

When conjugated with Sulfo-Cyanine 7.5 NHS ester dissolved in ultrapure water, exosomes were perfectly conjugated with the fluorescent probes being detectable by flow cytometry and confocal microscopy; furthermore, the exosomes presented a greenish colour at naked eye after the purification with the columns, sign of the incorporation of the dye (left samples for each image in Fig. 11).

4.3.1. Characterization of conjugated exosomes

To ensure that the conjugation with Sulfo-Cyanine 7.5 NHS ester was not destructive or causing noticeable alterations in the exosomal membrane or core size, TEM images and flow cytometry analysis of pasteurised milk-derived exosomes were evaluated.

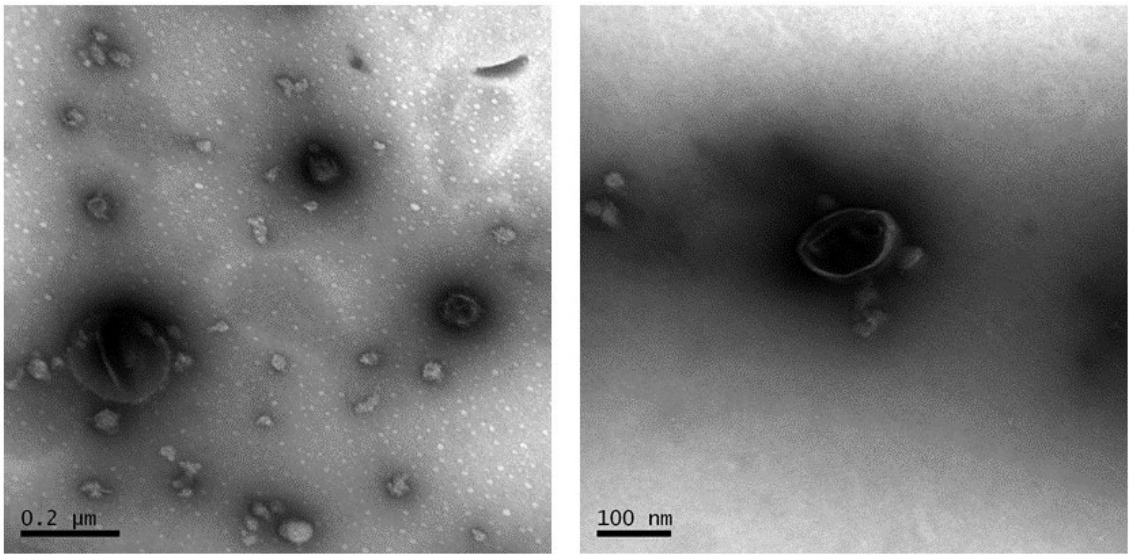

Fig. 12. Transmission electron microscopy of exosomes conjugated with Sulfo-Cyanine 7.5 NHS ester. Images were visualized using 100,000 x and 150,000 x magnification, respectively.

Isolated exosomes of different sizes can be observed on Fig. 12, with their characteristic cup-shape. The only observable difference between blank and functionalized samples is the intensity of the dark staining caused by negative staining of TEM. No major effects were observed in shape or size of fluorescently labelled exosomes.

When analysed by flow cytometry, similar patterns in terms of size and complexity were obtained for blank and conjugated exosomes.

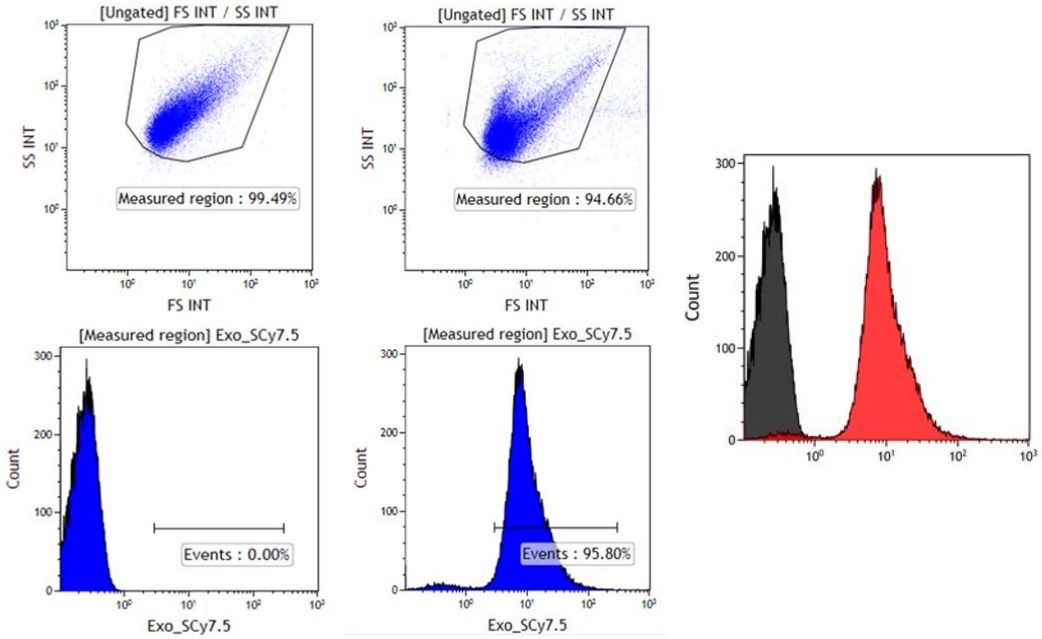

Fig. 13. Flow cytometry analysis of conjugation of Sulfo-Cyanine 7.5 NHS ester with the surface of exosomes derived from pasteurised milk. Population and fluorescent event distribution (left panel) and overlay of fluorescent events (right panel).

Between 30,000 and 40,000 events were measured for each of the samples. Both control and functionalized exosomes showed similar population distribution (Fig. 13 left panel). Blank (control) exosomes presented no fluorescence when compared with conjugated exosomes, which exhibited a 95.80% of fluorescent events with intensity high enough to make the two populations distinguishable (right panel). Less than a 5% of stained samples showed no fluorescence. Similar results were obtained for samples that were frozen after their conjugation.

4.4. *In vivo* biodistribution in healthy animal

The examination of ex vivo imaging of organs (seen in Fig. 14) indicates that the biodistribution in healthy animal of free Sulfo-Cyanine and conjugated exosomes is different. Free dye is mostly accumulated (73%) in small and large intestines, kidneys (13%) and liver (9%). With respect to the exosomes, they tend to gather in liver (60%), kidneys (23%) and intestines (16%). Free Sulfo-Cyanine goes directly to the secretory pathway while exosomes are gathered in liver. The right image presents an illumination artifact in the bottom right corner.

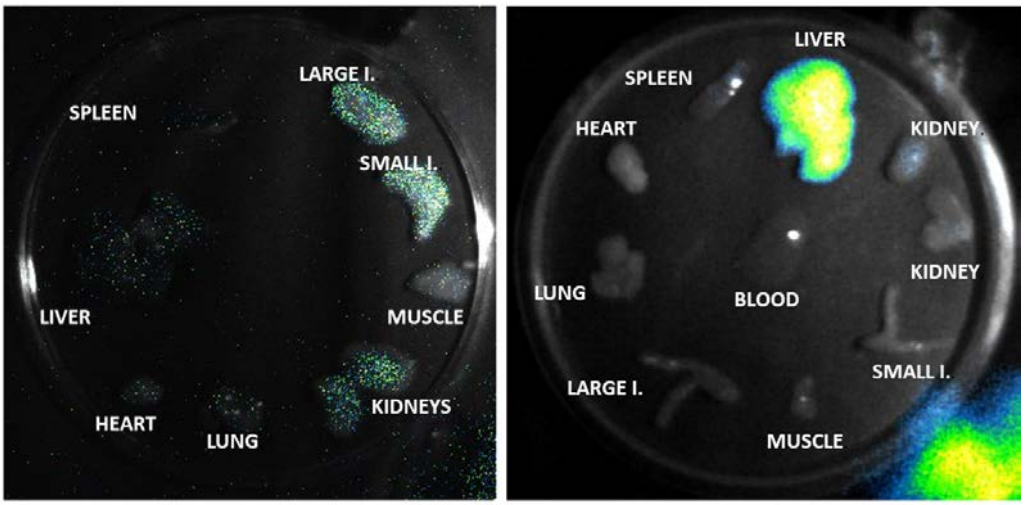

Fig. 14. Ex vivo imaging of accumulation of free dye (left) and conjugated exosomes (right) in organs of healthy mice.

4.5. Cell culture

Culture of tumour-derived cells (B16F10, HeLa and U87) and primary hepatocytes was successfully performed as explained in the Methodology. High confluences were obtained and growth of cells in different culture plaques (24- or 96-wells, Flasks75, Petri dishes) was possible without affecting the morphology or characteristics of the cells.

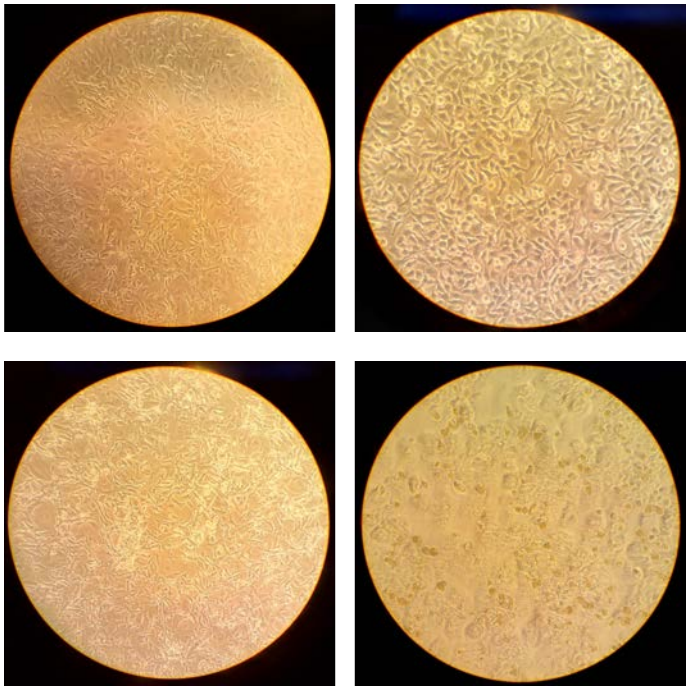

Fig. 15. Highly confluent cells of the different cell types cultivated. From left to right, top: B16F10, HeLa; bottom: U87, hepatocytes.

4.6. Validation of the conjugation technique

4.6.1. Isolation of cancer exosomes

Exosomes derived from cancer cells were isolated, conjugated and characterized. Three different samples were analysed, one of each type of cancer cell exosomes (B16F10, HeLa and U87). After the protein content analysis, non-homogeneous results in the protein content between the different samples were observed: for HeLa, 28 ± 10 μg were obtained per 30 ml, while for U87, the isolation process yielded 83 ± 3 μg. In the case of B16F10, the extraction yielded 43 ± 9 μg.

When analysing the size distribution, all the exosomes (Exo-Hela, Exo-U87 and Exo-B16F10) presented consistent size within the range of exosomes (Fig. 16), with broader distribution in comparison with commercial milk exosomes and similarities to the distribution of natural milk-derived exosomes. B16F10 and U87 exosome present similar distributions, while HeLa has a wider distribution with the appearance of a small peak in the range of 20 nm, indicating the presence of destroyed exosomes and small proteins. The typical exosome size for the different cell lines are: 177 ± 13 nm (n=2) for B16F10, 237.5 ± 17.5 nm (n=2) for HeLa and 143 ± 21 nm (n=2).

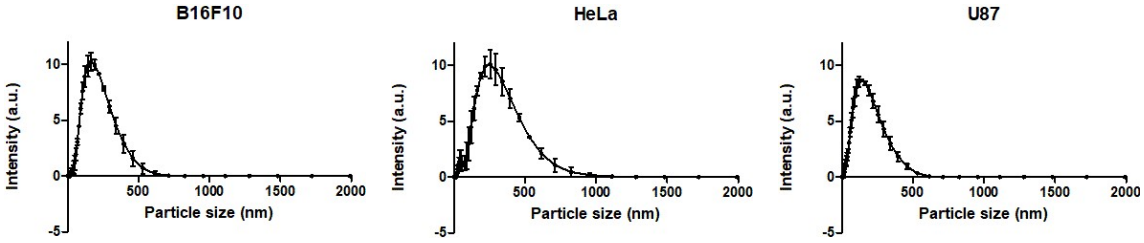

Fig. 16. Hydrodynamic size distributions of cancer cells-derived exosomes corresponding from top to bottom to B16F10, HeLa and U87 exosomes.

U87 exosomes appear to be the smallest in size with the size distribution more shifted to the left, and those derived from HeLa the largest ones as well as the most destroyed ones; this is consistent with the typical exosome size.

4.6.2. Conjugation of cancer exosomes with fluorophores

For the flow cytometry, a gate separating two different populations, one more concentrated containing smaller events and other with a broader size distribution of bigger events were defined. It was observed that all samples, both labelled and blank, fulfilled the gate for population distribution except the control blank exosomes obtained from HeLa (Fig. 17 top panel), which presented an increased population of events with smaller size than the

traditional diameter of exosomes. Furthermore, fewer events were detected in the labelled exosomes in comparison with the blank samples.

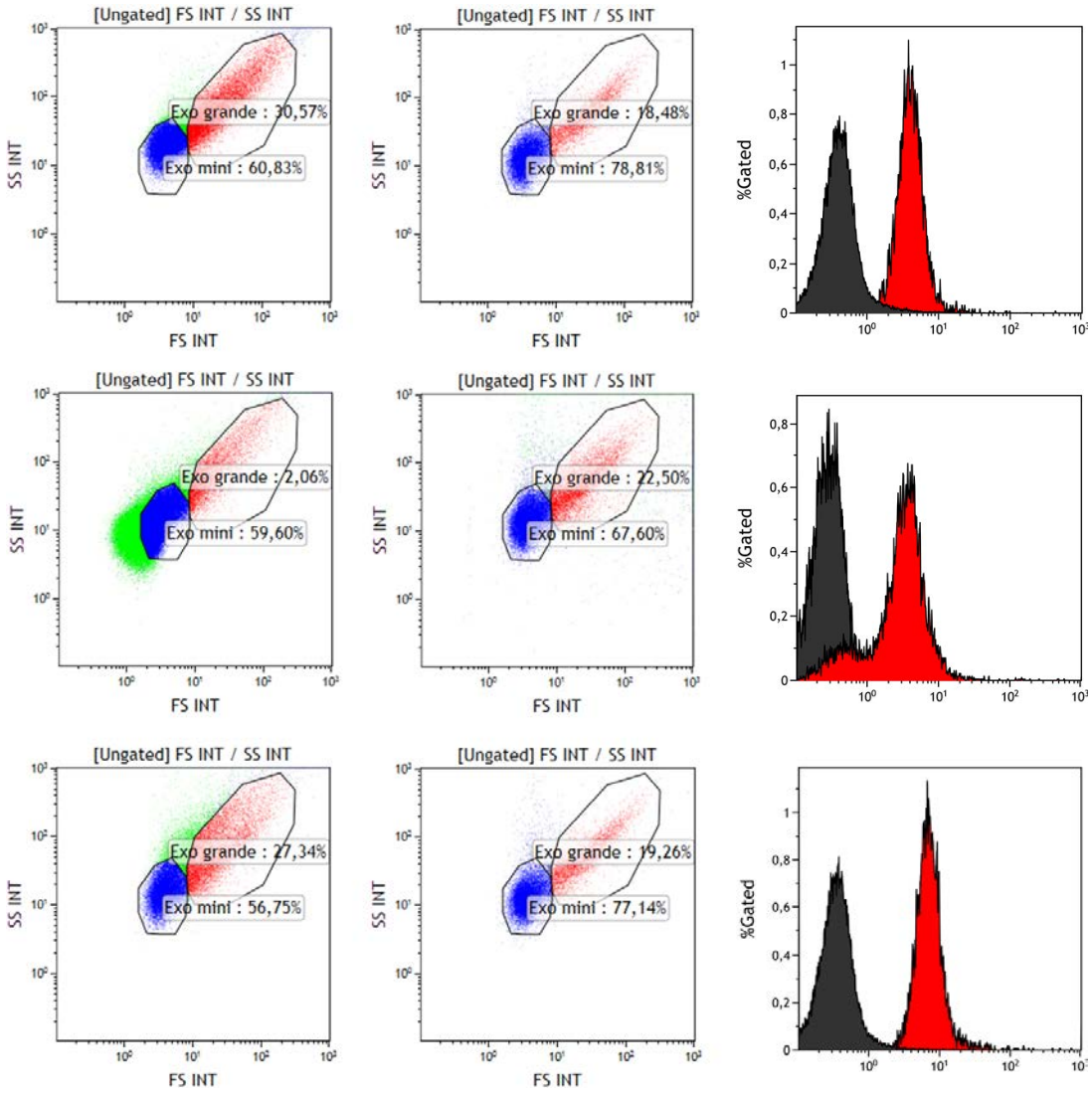

Fig. 17. Flow cytometry analysis of blank and fluorescently labelled exosomes in the near infrared spectrum. Population distribution and the designed gates (left panels). Overlay of fluorescent events from control and conjugated exosomes (right panel). From top to bottom, rows correspond to B16F10, HeLa and U87 exosomes.

When analysing the differences in fluorescence (Fig. 17 right panel), blank exosomes present a minimum fluorescent signal, while exosomes conjugated with near-infrared dye show intense fluorescence. Exosomes from U87 and B16F10 present a high percentage of fluorescent events, indicating than more than the 99% of the exosomes are marked; for Hela-derived exosomes, this percentage is reduced to 83%, showing some small-sized events that did not get stained.

Size and morphology of exosomes were examined in order to determine the belonging of the obtained vesicles to the exosome category. As goat's milk exosomes and others reported in literature, tumoral exosomes presented rounded cup-shape with negative staining, of congruent sizes for both stained and unlabelled samples of all tumoral cell lines.

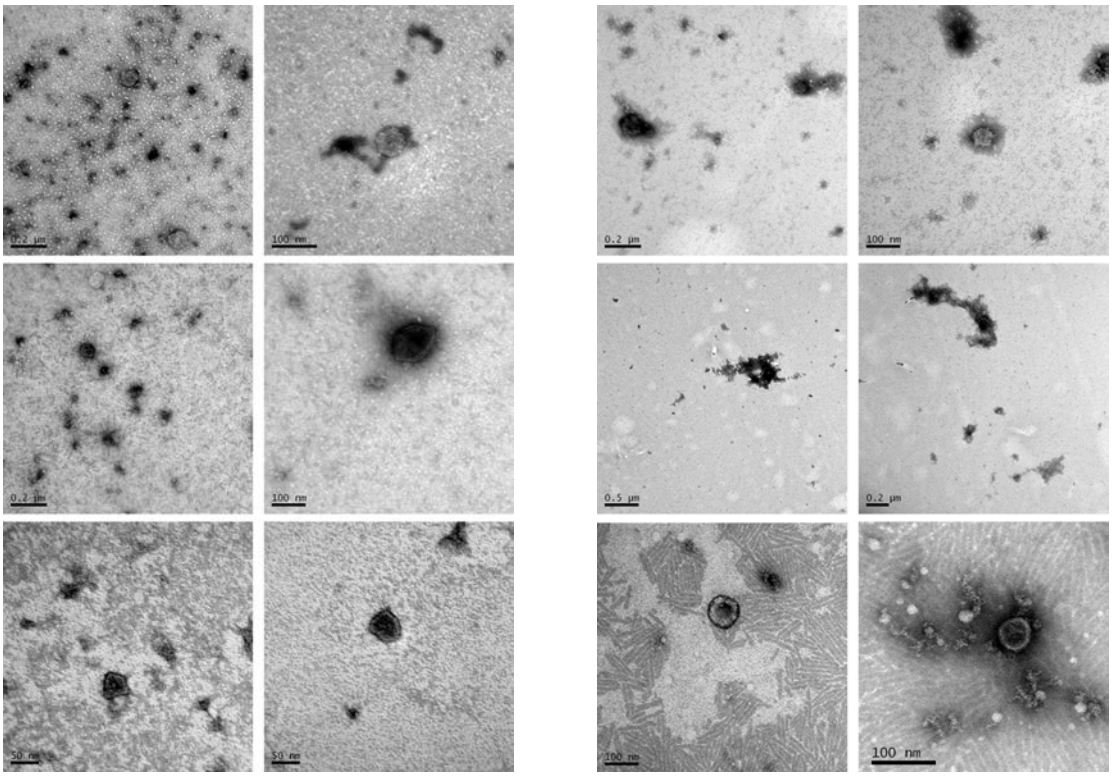

(a) (b)

Fig. 18. Comparison of TEM images of the treatment of tumoral cells with blank (a: control, left panel) and conjugated (b: right panel) exosomes. From top to bottom, the inspected cells are B16F10, HeLa and U87.

Images from unlabelled exosomes can be seen in the left panel and those of functionalized exosomes in the right panel; for both, rows correspond from top to bottom to B16F10, HeLa and U87 cells respectively. No observable differences are appreciated between left and right panels. Additionally, HeLa exosomes appeared destroyed, being congruent with the results obtained from flow cytometry analysis, in which unstained peaks were observable as well as a reduced number of events once labelled.

4.7. *In vitro* toxicity assessment

To investigate the short-term toxicity of exosomes in cancer and hepatic cells, these were treated with blank exosomes derived from pasteurised milk (to avoid any effect of the NIR dye to the absorbance measurement) at various concentrations (0-20 μg/ml) and the

viability was tested with MTT assay at 24 and 48 hours from the dose addition.

Concentrations of 0 (control), 0.05, 0.5, 5 and 20 μg/ml doses were added to hepatocytes cultured *in vitro* for at least 24 hours from the liver extraction (according to section 3.9 from Methodology). Absorbance was measured at 595 nm and results were normalized with respect to the null dose.

At 24 hours it is observed that absorbance (and therefore the viability of cells) is slightly below the zero value (Fig. 19 left panel). The increase in the exosome dose does not appear to have any effect on the viability of hepatocytes. A small increase in the absorbance can be observed for the higher dose. At 48 hours similar results are obtained, with the viability maintained constant at the zero value for all concentrations (Fig. 19 right panel).

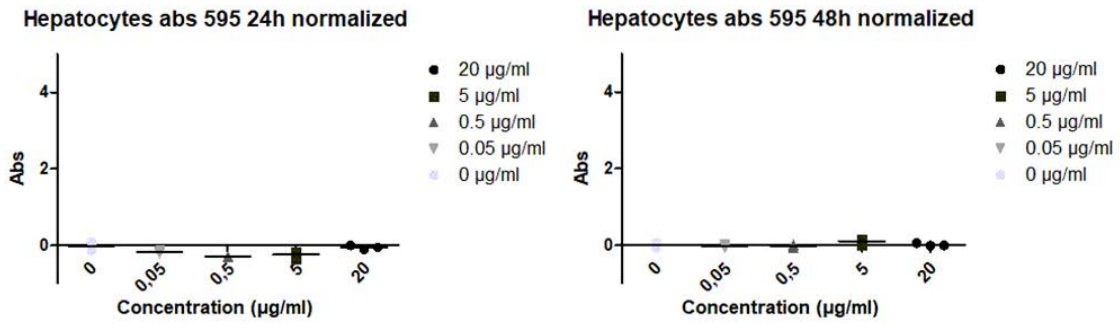

Fig. 19. Hepatic cells were treated *in vitro* with differential doses (0-20 μg/ml) to test short-term toxicity (at 24 and 48 hours) of exosomes using MTT assay.

Visual inspection of cells using light contrast microscope provided no further information, as the number of living cells was high and no cell death was obvious at naked eye. No significant toxicity nor observable effects in the number and morphology of cells were found.

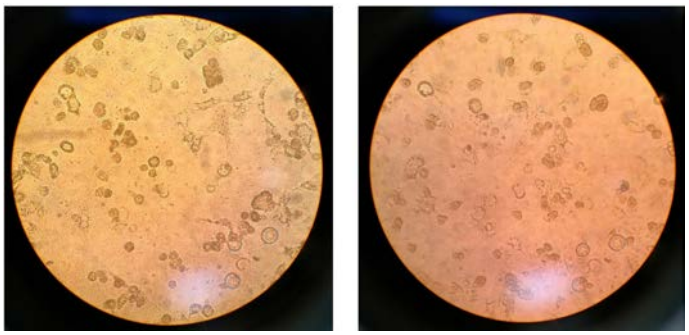

Fig. 20. Visual inspection of hepatocytes at 48 hours after the addition of 0 μg/ml (control, left image) and 5 μg/ml (right image) of blank exosomes.

An additional MTT assay was performed to analyse the toxicity of exosomes in cancer cells (mouse melanoma B16F10, human adenocarcinoma HeLa and human glioblastoma U87). Doses between 0 and 20 μg/ml were used and the absorbance caused by cellular activity was measured; additionally, the absorbance of the different doses of exosomes in culture media was analysed.

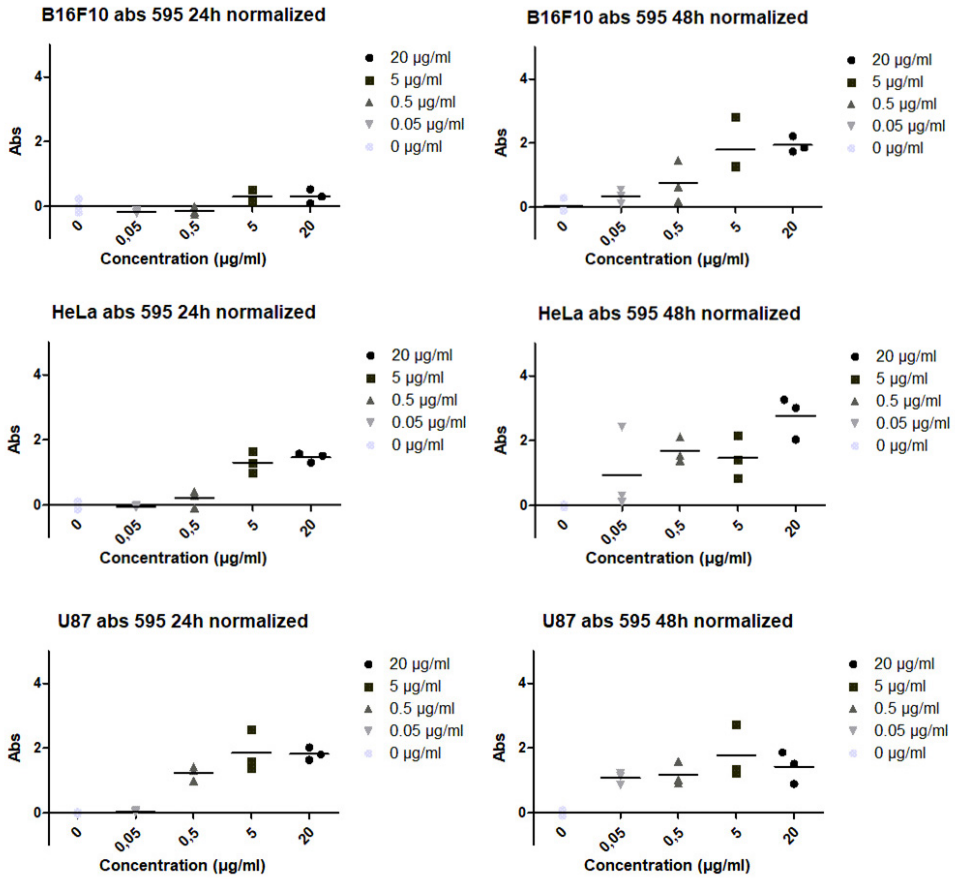

Fig. 21. Analysis of viability of cancer cells treated *in vitro* with differential doses (0-20 μg/ml) to test short-term toxicity (at 24 and 48 hours for left and right panels respectively) of exosomes using MTT assay. From top to bottom, rows correspond to B16F10, HeLa and U87 exosomes.

At 24 hours (Fig. 21 left panel), for B16F10 cells, absorbance was close to the zero value for lower doses. For the highest ones it was slightly over zero. In the case of HeLa, same results were obtained for 0.05 and 0.5 μg/ml doses, while the increase in the highest ones is more noticeable. With respect to U87, only the lowest dose is close to zero, while the other three (0.5, 5 and 20 μg/ml) show important increases in absorbance.

At 48 hours (Fig. 21 right panel), less homogeneous values are obtained, in general showing an increasing absorbance when the dose is incremented. The exceptions are the 5 μg/ml doses of HeLa (being its absorbance lower than the 0.5 μg/ml dose) and U87 (showing an unexpected higher value than the highest dose).

Additionally, visual inspection of cells was performed at 48 hours before the MTT assay (Fig. 22), for B16F10 showing how cells of wells where high doses had been applied (5 and 20 μg/ml) were totally destroyed, while for 0.5 and 0.05 μg/ml cells appeared to have strange morphologies and presented aggregation. In the case of HeLa, cells of higher doses were barely visible, rounded or destroyed, while at 0.5 μg/ml and 0.05 μg/ml they presented aggregation and abnormal morphology. For U87, cells from 20 μg/ml wells were destroyed; 5 μg/ml and 0.5 μg/ml presented rounded morphology and aggregation, and 0.05 μg/ml appeared to be unaffected. Cells of wells with no dose presented normal morphology and growth, covering the whole bottom of the well (similar to those in Fig. 15).

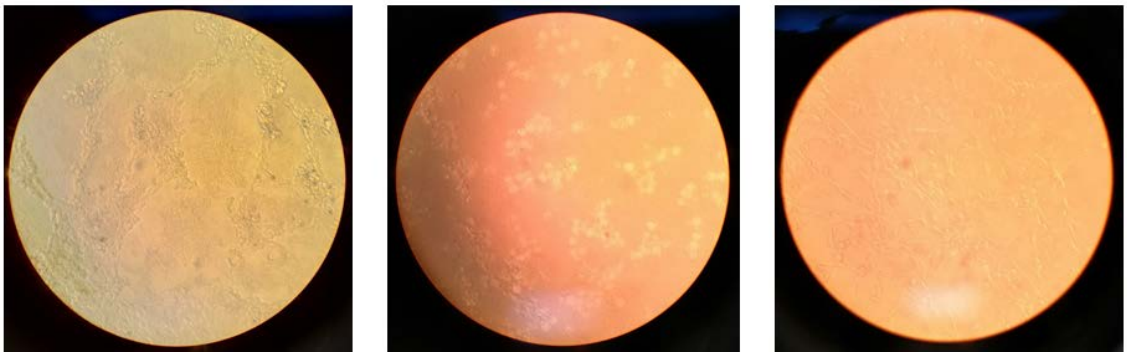

Fig. 22. Visual inspection of cancer cells at 48 hours after the addition of exosomes.

To analyse whether this effect may be caused by interference of exosomes with the MTT assay, the absorbance of exosomes in medium with collagen (with no cells seeded) was also measured (Fig. 23). At 24 hours, doses of 5 μg/ml and 20 μg/ml rendered high unforeseen absorbances, in comparison with the lowest doses that did not present any absorbance (as expected). For measurements taken at 48 hours, absorbance was detectable for all concentrations.

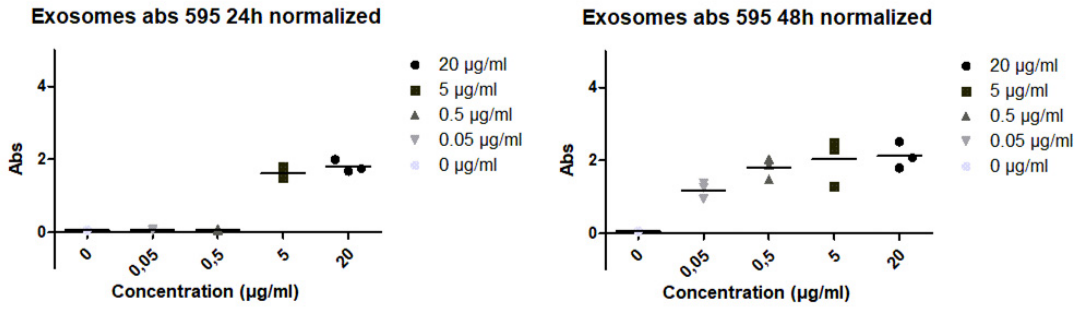

Fig. 23. Measurement of the absorbances of exosomes seeded in medium with collagen for different dose concentration (0-20 μg/ml) and periods of time (24 and 48 hours).

Moreover, when the wells containing only exosomes on medium with collagen-covered bottom were observed through the microscope, the bottom of the well appeared to be cov-

ered by a rough network of higher density for the higher doses. Wells containing only collagen and medium did not present this “carpet”, seen in Fig. 24.

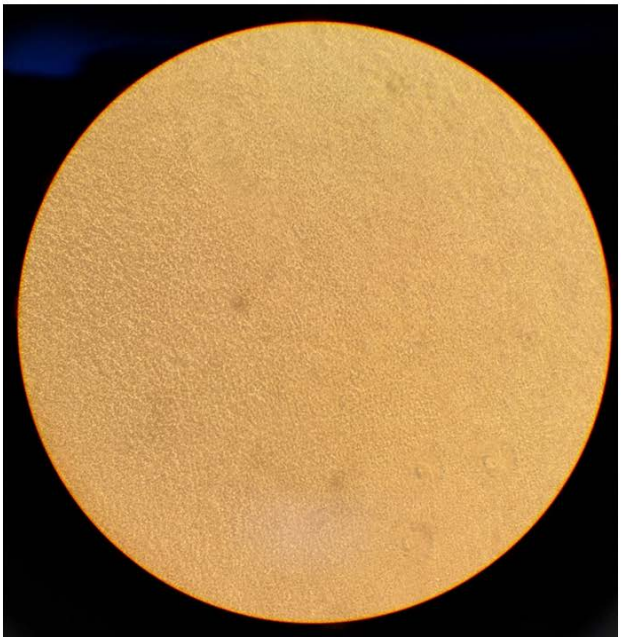

Fig. 24. Visual inspection of wells containing exosomes in medium with collagen at 48 hours after the addition of blank exosomes.

4.8. *In vitro* uptake studies

To investigate the *in vitro* cell uptake of pasteurised milk-derived exosomes, mouse melanoma B16F10 cells, human adenocarcinoma HeLa cells and human glioblastoma U87 cells were treated with Sulfo-Cyanine7.5-conjugated exosomes at various concentrations (0.5 and 5 μg/ml) and durations (0.5-24 hours).

The cellular internalization of exosomes was examined using confocal microscopy; no significant uptake was detected at any time for B16F10 neither HeLa cancer cells (top panel of Fig. 25). On the contrary, a time-dependent increase was observed for U87 cells (bottom panel of Fig. 25). Similarly, the higher concentration presented higher uptake during time, being the uptake for the lower dose almost unnoticeable for all cell lines.

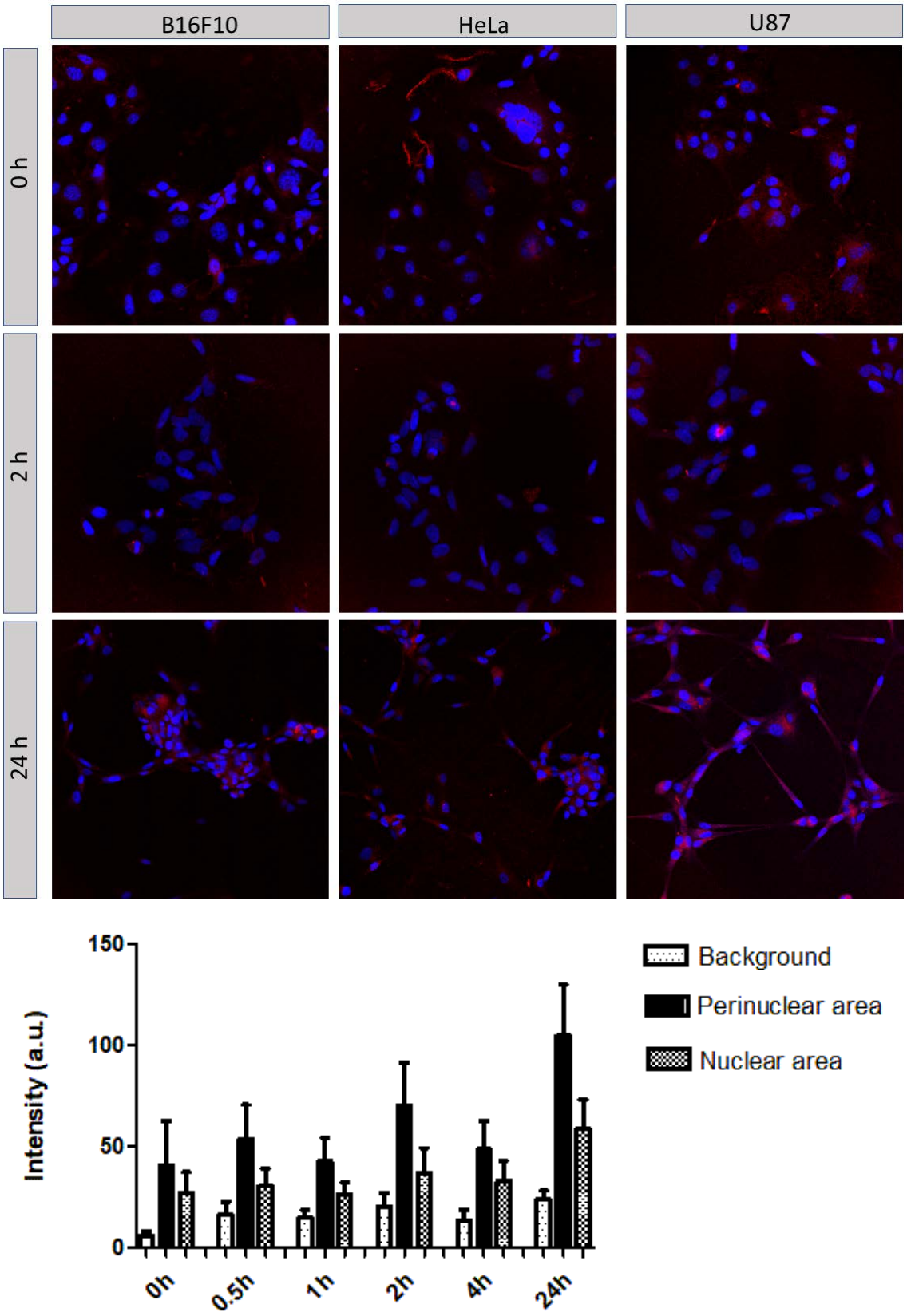

Fig. 25. Uptake of milk exosomes by cancer cells. (A) Confocal images of uptake experienced by the different cells at different time points for 5 μg/ml. (B) Quantification of fluorescent intensity, showing a time-dependency for U87 cells with dose 5 μg/ml.

Different areas of the cells were evaluated, revealing that exosomes tend to localize non-uniformly inside the cells, as the perinuclear region presented higher intensities than the distal regions of the membrane and the nucleus (bottom panel of Fig 25). The localization of exosomes in the perinuclear area is quantified, being congruent with the tendency observed in the confocal images. The time dependency with respect to the intensity observed for U87 cells at higher dose does not present any linearity, but a general exponential behaviour in which increased intensity in the near infrared channel is observable.

5. DISCUSSION

The focus of this Bachelor Thesis was the evaluation of goat's milk-derived exosomes as a new theragnostic platform in oncology, due to the particular characteristics of lipidic membranes of exosomes that allow their use as substitute of liposomes. To do so, the viability of goat's milk as source of exosomes and the hypothesis stated (such as the lack of toxicity or tumorgenicity) had to be confirmed.

Due to the enormous variety of exosomes present in different biological samples, several extraction methods can be found in literature to maximize the yield and purity and reduce the destruction of exosomes depending on the complexity of the method and the biological sample from which exosomes are obtained. Some of these methods are based on physicochemical properties such as differential centrifugation, filtration or density gradients, while others exploit biochemical reactions. The presented protocol combines both physico- and biochemical processes, using differential ultracentrifugation, size-exclusion chromatography and curdling agent to optimize the purity of the obtained exosomes. Using this optimized protocol and selecting the appropriate milk, the protein content is reduced to its minimum and the yield of pure exosomes is maximized.

Additionally, exosomes from goat's milk, either commercial skimmed pasteurised or direct from the goat, not treated, were characterized to evaluate which one is more suitable for research purposes. Being both visually identified as exosomes with Transmission Electron Microscopy as exosomes, showing the characteristic cup-shape and being in the size range and morphology typical of exosomes according to literature, it can be concluded that the aforementioned protocol allows the isolation of purified and intact exosomes in high yields.

Depending on their origin, milk exosomes show distinct characteristics, mainly differences in the hydrodynamic size distribution and the protein content. The amount of protein in micro-grams of fresh unpasteurised milk doubles the protein concentration obtained from commercial skimmed pasteurised milk, indicating that the pasteurisation, skim and treatments performed in the dairy industry reduces notably the exosome content of the samples. Additionally, exosomes of different sizes are identifiable in TEM images of untreated milk, which agrees with the broader hydrodynamic size distribution of exosomes obtained from these samples, which implies a higher heterogeneity in size. This is caused by vesicles gathering in accumulation of exosomes embedded in proteins, due to the increased protein content of these samples. This aggregation of higher number of exosomes diverse in size is not appreciable for pasteurised milk-derived exosomes. Thus, DLS results are consistent with the information extracted from the TEM images, which

showed the differences in size between the exosomes derived from the distinct milks and indicates that the broader size distribution for unpasteurised milk is caused by aggregations of exosomes. The exosome size was therefore confirmed to be within the range of 50-200 nm stated in literature.

The comparison between commercial and fresh natural milk was carried out in order to determine the optimal source for the stated purposes; it was observed that skim pasteurisation at 72ºC did not cause destruction of the exosomes, but rather eliminated undesired proteins from the samples. Although the protein content and the number of exosomes appears to be significantly lower in the commercial milk, its availability at regular stores, its size homogeneity and lower amount of contaminant proteins makes it more suitable for scientific research.

Since one of the intentions of this Thesis is to use exosomes as natural liposomes in oncology using optic imaging *in vivo*, exosomes needed to be functionalized with fluorophores, as they don't naturally present fluorescence. Probes in the near-infrared range were used to avoid interference caused by the autofluorescence of tissues and to prevent the loss of absorption by tissues.

There already exist commercial kits that functionalize exosomes based on their hydrophobicity, coating the vesicle with a thin-layer of dye maintained with weak bonds that are easily degraded, not being resistant to the different processes to which exosomes are subjected when used as theragnostic platform *in vivo*. Due to this lack, a chemical tool for robust conjugation of exosomes was developed and optimized by exploiting the covalent bonds that can be formed between the lipidic membrane of exosomes and the selected NHS ester dyes. This strong covalent bond stablished between the fluorophore and the exosome will avoid possible false positives caused by the detachment of the dye from the vesicle and allowing the tracking of the exosome over time and different conditions. As far as I know, there is no bibliography regarding the covalent conjugation of exosomes with fluorophores *in vivo*, being this work the firs approach developed in the covalent conjugation of exosomes.

Exosomes were conjugated with Cyanine and Sulfo-Cyanine 7.5 NHS ester. The differences between them consist on the sulfo groups present in the Sulfo-Cyanine, which makes the dye hydrosoluble instead of soluble in organic solvents as Dimethyl Sulfoxide, which has proved to destroy the exosomes.

Characterization of functionalized exosomes showed a high yield in the conjugation, indicating that exosomes can be robustly conjugated with NHS ester fluorophores. Additionally, the chemistry does not alter the membrane nor destroy the exosome, as TEM and

flow cytometry analysis confirmed. No significant differences in shape, size, complexity, general aspect or function between stained and blank exosomes were found; the only observable difference between blank and dyed samples is the intensity of the dark staining caused by negative staining of TEM. This could be caused by a slight change in the Zeta potential, which changed from -12.57 ± 0.58 mV to -11.93 ± 0.047 mV.

From the characterization, it can be deduced that the exosomes are resistant enough so that they are not degraded by the chemistry of conjugation and the purification with exo spin columns. Additionally, the fluorescent signal, situated in the near infrared spectrum, is strong enough to allow its detection not only *in vitro* experiments but also *in vivo* in healthy animals. From this experiment, which was carried out without my participation, it was demonstrated the different pathways undergone by free dye and labelled exosomes. This consistently demonstrates that the labelling does not affect the biodistribution of exosomes, as they notably accumulate in liver (60% of uptake in comparison with 23% of kidneys) as reported on literature [15].

Furthermore, the verification of robustness of the conjugation method for different and less resistant exosomes was accomplished. For this, the isolation, characterization and labelling of tumoral exosomes was carried out following similar procedures as those stated in the Methodology section except for the isolation, which was performed using a simplified differential centrifugation protocol with no purification steps.

The advantages of performing this validation in cancer exosomes is not only the aforementioned, but also a comprehensive understand about the physicochemical characteristics of tumoral exosomes may help researchers to discern pathways or related mechanisms of the metastatic processes, since exosomes have proved to be involved in pro-oncogenic and metastatic processes, altering the tumour microenvironment and exchanging information for tissue preparation prior colonization. Additionally, the presence of these extracellular vesicles in body fluids have been used as biomarkers of the disease; the possibility of tracking the position of tumoral exosomes within the body in real time using molecular imaging opens the door to diagnosis of metastasis before its actual appearance, and would improve our understanding on tumour development.

The non-homogeneous results obtained regarding the protein content between the different samples were possibly due to the number of cellular passages that the cells had been subjected and the number of days of culture before the medium was retired. More extractions would be required to establish if the variations between the protein content in micrograms was due to the aforementioned differences in cellular stage, or caused by intrinsic differences in the exosomal production between the distinct cell types.

The differences between the fulfilment of the gates regarding the population distribution for blank and conjugated exosomes lead to the conclusion that the labelling or the exo spin columns are affecting the exosome or, at least, reducing the impurities. These differences in size between the types of exosomes are also observable in TEM images, due to the differences in the species of origin and cell type. Still, their morphologies and sizes are ranging between those described in literature, being possible to affirm that the reported nanovesicles are indeed exosomes derived from tumoral cells.

More numerous signs of destruction were found in the characterization of these exosomes than those observed for milk-derived exosomes, confirming the hypothesis that cancer exosomes are less resistant than milk ones, since they are more destroyed with a less aggressive isolation process. Despite their fragility, blank and labelled exosomes were analysed by TEM and flow cytometry; with the exception of HeLa exosomes, they were satisfactorily isolated and conjugated, showing the characteristic cup-shape and size range and allowing their confirmation as exosomes. Additionally, the overlay of flow cytometry analysis indicates that exosomes are labelled in more than a 99% of cases for B16F10 and U87, while only an 85% of conjugation was obtained for HeLa. This is consistent with the fact that HeLa exosomes were destroyed, as seen in the TEM images and in the hydrodynamic size distribution. This may indicate that only exosomes are being conjugated, but in any case, it is a sign of the robustness of the conjugation technique, which allows the functionalization of even delicate exosomes.

The capability of tumoral exosomes to be conjugated with the proposed optical dye with satisfactory results is demonstrated; among the different studied types, those derived from U87 cells appear to be the ones with better efficiency. The implications of this conjugation are mainly its use in molecular imaging, which could provide important insights into the biodistribution of tumoral exosomes and supply valuable information about the future behaviour of the primary tumour and possible metastasis.

As exosomes are proposed as natural, non-toxic liposomes, their toxicity was tested in both host cells (hepatocytes directly obtained from euthanized animals) and different tumour models. Between the diverse assays to determine toxicity and viability, a tetrazolium assay (concretely MTT) was selected due to its reduced price, its suitability for high throughput screening and its non-radioactivity. This technique is based on the reduction of MTT substrate into purple-coloured formazan by cells with active metabolism being the colour a marker of viability of the cells.

Hepatocytes showed nearly unaltered absorbances, and thus, unaffected proliferation and viability with respect to the control, indicating that exosomes do not harm host cells where the uptake is greater in healthy animal. This was checked by visual inspection of

the cells at 48 hours; since no observable differences were remarkable, it can be assumed that the above hypothesis is true. In the case of cancer cells, absorbance values were different from cero, especially for 48 hours; this may indicate that exosomes benefit proliferation of cancer cells, but visualization with light phase microscope shows destruction or, at least, substantial abnormalities in morphology, number and distribution, signifying that exosomes present an anti-oncogenic behaviour rather than causing their proliferation. This destructive effect was not observed in the control wells, where no dose had been added, indicating that this disaggregation of the tumour environment was caused by the goat's milk-derived exosomes.

The hypothesis that explains this discrepancy between the MTT assay results (which suggest that the viability and proliferation of cancer cells is incremented by the addition of exosomes) and the information retrieved by visual inspection (which support that exosomes cause some grade of disruption of normal behaviour of cancer cells) suggest that exosomes have some sort of pseudo-cellular behaviour, presenting metabolic activity and causing reduction of the MTT substrate. To check this, a separate study only with different concentrations of exosomes was carried out; it was observed that increased absorbance values were measured, coinciding exactly with the high absorbance measured for cancer cells. This consistency indicates that the absorbance measured when the cells were destroyed was indeed caused by the exosomes, which are deposited in the collagen-covered bottom. The collagen itself cannot be the cause of the interference since controls did not presented any incremented absorbance.

In order to further analyse these findings, additional experiments were designed to perform MTT assay on half of the cells and confocal microscopy analysis of the other half at both 24 and 48 hours, in an attempt to identify the causes of such differentiated effects on healthy and aberrant cells. These would have probably been the next steps in the research.

The uptake ability of tumour-derived cells was examined in order to determine the possibility of success of accumulation of the fluorescent probe in tumours *in vivo* experiments. Although the Enhanced Permeability and Retention effect allows the hypothetic gathering of nanosized vesicles in the tumour, this accumulation would be strongly increased by the tendency of the tumour itself to uptake nanoparticles. Exosomes have been demonstrated in literature to be able to be internalized by cells [36], being this effect extremely desirable to use the exosomes as drug carriers for oncologic therapy. It was observed that the different cell lines respond differently to exosomes, being the glioblastoma U87 cells the only ones presenting noticeable uptake denoted by a detectable increased intensity in the near infrared channel.

Going into details, for the evaluation in tumour model, the uptake study was carried

out in order to select the most appropriate cancer cell line to be translated into an in vivo model. The behaviour of exosomes was evaluated in the same cancer cell lunes that were used in the toxicity assessment. Since the platform was designed as theragnostic platform, the distribution at cellular level results of high relevance; for this, different areas were evaluated, leading to the conclusion that uptake of exosomes by cells mainly takes place at the perinuclear area of the cytoplasm rather than inside the nucleus; this is consistent with literature [15]. While several problems were encountered with the autofluorescence of cancer cells, even in the near infrared spectrum, differences in the intensity (and therefore in the uptake of NIR fluorescent by the distinct cell types) were observed at several time points and concentrations. In general, it was observed a dependency between the concentration of the dose and the intensity measured, such as that the higher the dose, the more incremented the intensity.

6. FRAMEWORKS

6.1. Socioeconomic framework

Malignant tumours, together with diseases of the circulatory system, are the two leading causes of death in the world. Specifically, in Spain during 2016, they represented the 26,8% and 29,7% respectively, according to the 'Reporte Anual del Sistema Nacional de Salud 2016' [53], developed annually by the Spanish Government. The mortality caused by cancer was of 112,939 deceases during the aforementioned year; among the different types of cancer, colon, prostate, lung and breast cancer are the most common.

In an attempt to identify the economic impact of this disease, several terms must be defined [54] [55]:

- Direct costs: they represent the value of the resources from the National System of Health required to prevent, detect and treat a health problem. They are constituted by the primary attention, hospital and anti-cancer drugs costs.
- Indirect costs: referred to the value lost by the lack of productivity occasioned by the disability or death of the patient. In this section, costs derived of the informal care – that is, the attention received by a person with limited autonomy to perform their daily tasks – is also included.
- Intangible costs: related to the non-monetary consequences of the disease, like the pain.

The estimation methods of these costs are mainly two, which can yield very differentiated results:

- Human-capital: it considers the patient's perspective, counting any hour not worked as a lost one.
- Friction-cost: it takes the employer's perspective as it contemplates as lost hours only those that have not been worked, until another employee substitutes the patient and carries out their work.

For the analysis of the economic impact in this thesis, the human-capital method will be used; the intangible costs were not included. Using the selected human-capital method, the total costs of malignant tumours during 2015 in Spain were 12,216 million of euros,

being a 60% of them derived from indirect costs. This figure represents the 11.3% of the Gross Domestic Product of the country during that year, and accounted for a 17% of the total sanitary costs (calculations performed with data obtained from the AnnualSpanish National Health Report [53].

As it can be seen in the aforementioned report, the economic impact of cancer in Spain each year is enormous. It is required the development of a system that would allow the early detection of primary and metastatic tumours; this premature diagnosis increments the survival rate of patients and thus, reduces the costs associated with loss of productivity. Moreover, the improvement in diagnosis and therapy techniques against cancer will result in increased life expectancy and wealth for the patients, especially taking into account that the proposed theragnostic system is non-invasive and non-radioactive, which improves patient's quality of life [56]. Thus, the social impact of the exosomes used as nanocarriers produces a noticeable social impact that must be considered in light of the numbers provided.

An additional impact that may not result noteworthy at first sight, but in view of further exploitation plans acquires importance, is the ethical impact of both the investigation and the profiteering intention. For the research, goat's milk was used to obtain the exosomes, instead of human maternal milk as other papers use during their research [4]. Not using human products as basic materials during the development of this work supposes the inexistence of further ethical issues apart from those derived from the use of animal models and human tumour cells [57] (as well as the caprine milk and other animal products typically used in research), which will be itemised in next section.

This lack of human origin products facilitates the exploitation plan, which consists mainly on the commercialization of conjugated exosomes in optimized doses for direct injection at the hospital. The resulting product would be hospital-oriented, not for individual use at home; therefore, it would be supplied directly to the health service in a similar way that vaccines or other treatments do.

Being the exosomes an extremely versatile chemotherapeutic platform with a wide range of applications [50], different methods of utilization can be developed with these fluorescently labelled nanoparticles. Some of these applications could be the diagnostic of inflammatory processes or bacterial infections, or treatments based on the alteration of the exosomal cargo (as several papers have already suggested [15] [35]) for cancer therapy.

6.2. Regulatory framework

As biological experiments were necessary to carry out this project, several regulation sets concerning the risk prevention during laboratory activities are considered, according to the national Spanish laws:

- Real Decree 664/1997: related with the protection of workers against risks related with the exposure to biological reagents.
- Real Decree 83/1999: regulation of the production and management of biosanitary and cytotoxic residues in the autonomous region of Madrid.
- Real Decree 53/2013: by which the basic regulations applicable for the protection of animals used in experimentation and other scientific purposes, including teaching, are established.
- Real Decree 223/2004: regulation of the clinical trials with medicines.
- Law 28/2009: regarding the guarantees and the rational use of medicines and other sanitary products.
- Real Decree 577/2013: which regulates the pharmacovigilance of medicines for human use.

In order to apply for authorisation, it is essential to have the favorable reports of the ethics Committee on Animal experimentation at the centre and an autonomous community-enabled body for project evaluation. In addition, the staff who will participate in the experiments must be previously trained according to the RD 53/2013 and the Order ECC 566/2015."

6.3. Budget

The following section shows the budget associated with the research developed during the last months at the 'Unidad de Medicina y Cirugía Experimental' from the Gregorio Marañón Hospital. As other biomedical investigations, several expensive materials were required; these costs are separated according to the part of the experimental procedure they correspond, but only the final costs per section are showed; an itemisation of the costs per section can be found in the Appendix:

Section	*Total costs (€)*
Extraction	173.1
Purification	1,062.10
Characterization	1,081.00
Conjugation	988.90
Cell culture	1,412.92
Toxicity studies	189.16
Uptake studies	888.15
General laboratory supplies	2,272.60
Licenses and extra costs	6,786.00
Total	14,853.93

Table 2. Budget of the different sections of the research and total costs

7. CONCLUSIONS AND FUTURE PERSPECTIVES

7.1. Conclusion

Once the different methodologies, hypothesis and experiments have been itemised and evaluated throughout this dissertation, different conclusions and main ideas can be extracted, among them, the most important ones are the confirmation that goat's milk exosomes are satisfactorily isolated, purified and characterized for the first time with the proposed protocol.

Although the hypothesis of the ideality of exosomes as substitute of liposomes has not been fully developed, it can be affirmed that exosomes constitute a promising platform as natural replacement of artificial liposomes, especially in the area of oncology.

Additionally, the designed novel conjugation method of exosomes with fluorescent molecules is robust and allows the labelling of different types of exosomes with fluorophores for their use in optical imaging with a high yield (higher than 95%) and causing no modification of the properties of exosomes. This validates their use in molecular imaging as part of the optical techniques.

In vitro toxicity studies show that exosomes do not present toxicity against host cells (hepatocytes), but appear to destroy tumour cells. Furthermore, viability assay based on metabolic activity shows that exosomes present pseudo-cellular behaviour. These properties suppose that their use in oncology could be of great importance.

It has been confirmed that milk-derived exosomes present different behaviour in presence of distinct cancer cell lines, with the highest uptake in the is U87 cell line (glioblastoma). Moreover, exosomes extracted from different cancer cell lines show differentiated behaviour and physico-chemical properties depending on their origin. It can be then concluded that exosomes present differentiated behaviour in distinct circumstances, as well as acting differently in similar situations due to their variated origin.

In general, it can be affirmed that the main objective of the Thesis, that is, the evaluation of exosomes as new theragnostic platform in oncology, as well as the subobjectives stated to carry out this evaluation, have been satisfactorily performed, yielding robust and consistent results.

7.2. Future perspectives

Although this primary evaluation yielded solid conclusions, further research needs to be done in order to ensure a safe translation to the clinic and the oncologic area. The most important ones, in my consideration, are the evaluation of the pseudo-cellular behaviour of exosomes, which apart from noteworthy, could cause interference with the therapy treatments, and the analysis of the suggested anti-oncogenesis properties of exosomes.

The following step on this Thesis would have been, apart from the aforementioned, the translation to an subcutaneous *in vivo* model in small animal of glioblastoma in order to analyse the ability of exosomes to be recruited in tumours. Additionally, related with the use of exosomes as natural liposomes for therapy, the alteration of exosome active cargo for drug therapy has necessarily to be addressed.

APPENDIX

Item	*Quantity*	*Unit cost* |€|	*Total cost* |€|
Goat's milk	2 bottles	3.56	7.12
Ultracentrifuge tubes	1 pack of 6	165.98	165.98

Table 1. Budget for exosome extraction

Item	*Quantity*	*Unit cost* |€|	*Total cost* |€|
Curdling agent	1 bottle	5.50	5.50
PD-10 desalting columns	2 boxes of 30 units	286.80	573.60
0.44 μm filter	1 box 50 units	161.00	161.00
Exosome spin columns	2 boxes of 30 units	161.00	322.00

Table 2. Budget for purification

Item	*Quantity*	*Unit cost* |€|	*Total cost* |€|
Bovine Serum Albumin	1 bottle 100 g	463.00	463.00
Coomassie Blue	2 bottles	114.00	228.00
Cytometer session	5 hours	6.00	30.00
TEM session	10 hours	36.00	360.00

Table 3. Budget for characterization

Item	*Quantity*	*Unit cost* |€|	*Total cost* |€|
Cyanine 7.5 NHS ester	2 bottles of 5 mg	210.00	420.00
Sulfo-cyanine 7.5 NHS ester	2 bottles of 5 mg	275.00	550.00
Sodium Bicarbonate ($NaHCO_3$)	1 bottle 500 g	18.90	18.90

Table 4. Budget for conjugation

Item	*Quantity*	*Unit cost* |€|	*Total cost* |€|
Rapid flow filter units	1 box of 12 units	119.00	119.00
Culture plaques 24 wells	1 box of 50 units	171.10	171.10
Culture plaques 96 wells	1 box of 50 units	533.70	533.70
Disposable serological pipettes 10 ml	2 boxes of 30 units	161.00	322.00
Disposable serological pipettes 10 ml	2 boxes of 200 units	65.10	130.20
RPMI medium	4 bottles	16.03	64.12
DMEM medium	3 bottles	9.00	27.00
PBS for cell culture	3 bottles	18.90	56.70
Trypsin 10x	1 bottle 100 ml	25.10	25.10
FBS	1 bottle 100 ml	15.95	15.95
Glutamine	1 bottle 100 ml	15.85	15.85
DMSO	2 bottles	66.50	133.00
HeLa cells	1 vial	Ceded by Culture Unit from G.M. Hospital	-
U87 cells	2 vial	Ceded by Culture Unit from G.M. Hospital	-
Hepatocytes	4 vial	Ceded by Culture Unit from G.M. Hospital	-

Table 5. Budget for cell culture

Item	*Quantity*	*Unit cost* |€|	*Total cost* |€|
Thiazolyl Blue Tetrazolium Bromide (MTT)	1 bottle of 100 mg	16.16	16.16
0.22 μm filter	1 box of 50 units	173.00	173.00

Table 6. Budget for toxicity studies

Item	*Quantity*	*Unit cost* |€|	*Total cost* |€|
Confocal microscope session	8 hours	7.00	42.00
DAPI	1 bottle of 1 mg	9.90	9.90
Microscope slide	1 box of 100 units	31.60	31.60
Cover slip glass	1 bottle of 15 ml	63.60	63.60
DAKO Fluorescent Mounting media	1 bottle of 15 ml	92.00	92.00
Collagen type I from rat tail	1 bottle of 25 ml	210.00	210.00
Naubauer chamber	1 unit	200.00	200.20
Haemocytometer cover glasses	1 box 100 units	184.30	184.30
Trypan Blue	1 bottle 20 ml	10.30	10.30
Formaldehyde	1 bottle 250 ml	44.25	44.25

Table 7. Budget for the uptake studies

Item	*Quantity*	*Unit cost* |€|	*Total cost* |€|
Variable Volume Pipettors	Set of 3 spanning from 0.5 to 1000 μl	312.00	312.00
Pipette tips	15 boxes of 200 units	62.16	932.40
Falcon 50 ml	2 boxes 500 units	168.40	336.80
Falcon 15 ml	2 boxes 500 units	163.60	327.20
Parafilm	2 units	38.00	76.00
PBS tablets	1 box of 100 units	185.00	185.00
Eppendorf	2 boxes of 1000 units	45.60	91.20
pH test strips	1 box	12.00	12.00

Table 8. Budget for general laboratory supplies

Item	*Quantity*	*Unit cost* |€|	*Total cost* |€|
Matlab 2017.b	1 license	2000.00	2000.00
Computer with basic office software	1 device	540.00	540.00
Working hours	400 hours	10.00	4000.00
Prism 5	1 license	246.00	246.00
Image J	1 license	Free software	-
Microscope Imaging software	1 license	Free software	-

Table 9. Budget for licenses and extra costs

BIBLIOGRAPHY

[1] J. Ferlay, I. Soerjomataram, M. Ervik, R. Dikshit, S. Eser, and C. M. et al., "Cancer incidence and mortality worldwide: sources, methods and major patterns in globocan 2012," *International Journal of Cancer*, vol. 136, pp. E359–E386, 2015.

[2] M. Roser and H. Ritchie, "Cancer." `https://ourworldindata.org/cancer`, 2018. Published online at OurWorldInData.org; accessed 27-May-2018].

[3] A. C. Obenauf and J. Massagué, "Surviving at a distance: organ specific metastasis," *Trends Cancer*, vol. 1, pp. pages 76–91, 2015.

[4] C. Admyre, S. M. Johansson, K. R. Qazi, J.-J. Filén, R. Lahesmaa, M. Norman, E. P. A. Neve, A. Scheynius, and S. Gabrielsson, "Exosomes with immune modulatory features are present in human breast milk," *The Journal of Immunology*, vol. 179:3, pp. 1969–1978, 2007.

[5] M. Kesimer, M. Scull, B. Brighton, G. DeMaria, K. Burns, W. O'Neal, R. J. Pickles, and J. K. Sheehan, "Characterization of exosome-like vesicles released from human tracheobronchial ciliated epithelium: a possible role in innate defense," *The FASEB Journal*, vol. 23, pp. 1858–1868, 2009.

[6] J. Conde-Vancells, E. Gonzalez, S. C. Lu, J. M. Mato, and J. M. Falcon-Perez, "Overview of extracellular microvesicles in drug metabolism," *Expert Opinion on Drug Metabolism & Toxicology*, vol. 6:5, pp. 543–554, 2010.

[7] L. Barile and G. Vassalli, "Exosomes: Therapy delivery tools and biomarkers of diseases," *Pharmacology and Therapeutics Journal*, vol. 174, pp. 63–78, 2017.

[8] D. Ha, N. Ya, and V. Nadithe, "Exosomes as therapeutic drug carriers and delivery vehicles across biological membranes: current perspectives and future challenges," *Acta Pharmaceutica Sinica B Journal*, vol. 6:4, pp. 287–296, 2016.

[9] N. Kastelowitz and H. Yin, "Exosomes and microvesicles: Identification and targeting by particle size and lipid chemical probes," *Chembiochem*, vol. 15:7, pp. 923–928, 2016.

[10] S. E. Andaloussi, I. Mäger, X. O. Breakefield, and M. J. A. Wood, "Extracellular vesicles: biology and emerging therapeutic opportunities," *Nature Reviews Drug Discovery*, vol. 12, p. pages 347–357, 2013.

[11] G. R. Willis, S. Kourembanas, and S. A. Mitsialis, "Toward exosome-based therapeutics: Isolation, heterogeneity, and fit-for-purpose potency," *Frontiers in Cardiovascular Medicine*, vol. 4:63, 2017.

[12] P. Munson and A. Shukla, "Exosomes: Potential in cancer diagnosis and therapy," *Medicines*, vol. 2:4, pp. 310–327, 2015.

[13] E. Andaloussi, I. Mäger, X. Breakefield, and M. Wood, "Extracellular vesicles: biology and emerging therapeutic opportunities," *Nature Reviews Drug Discovery*, vol. 12:5, pp. 347–357, 2013.

[14]

[15] R. Munagala, F. Aqil, J. Jeyabalan, and R. C. Gupta, "Bovine milk-derived exosomes for drug delivery," *Cancer letters*, 2015.

[16] B. C.-S. et al., "Pancreatic cancer exosomes initiate pre-metastatic niche formation in the liver," *Nature Reviews Drug Discovery*, vol. 17:6, pp. 816–826, 2015.

[17] K. Chen and X. Chen, "Design and development of molecular imaging probes," *Current Topics in Medicinal Chemistry*, vol. 10:12, pp. 1227–1236, 2010.

[18] E. Kim, "Molecular imaging in oncology," *Journal of Nucelar Medicine*, vol. 54, pp. 1005–1420, 2013.

[19] R. Weissleder and U. Mahmood, "Molecular imaging," *Radiology Journal*, vol. 219, pp. 316–333, 2001.

[20] D. Margolis, J. Hoffman, R. Herfkens, R. Jeffrey, A. Quon, and S. Gambhir, "Molecular imaging techniques in body imaging," *Radiology Journal*, vol. 245, pp. 333–356, 2007.

[21] R. Weissleder, "Molecular imaging in cancer," *Science*, vol. 312, pp. 1167–1171, 2006.

[22] D. Mankoff, M. Farwell, A. Clark, and D. Pryma, "How imaging can impact clinical trial design: Molecular imaging as a biomarker for targeted cancer therapy," *Cancer Journal*, vol. 21:3, pp. 218–224, 2015.

[23] L. Fass, "Imaging and cancer: A review," *Molecular Oncology*, vol. 2:2, pp. 115–152, 2008.

[24] M. L. S.N. Histed, E. Mena, B. Turkbey, P. Choyke, and K. Kurdziel, "Review of functional/ anatomic imaging in oncology," *Nuclear Medicine Communications*, vol. 24533:4, pp. 349–361, 2012.

[25] E. Mena, M. Taghipour, S. Sheikhbahaei, S. Mirpour, J. Xiao, and R. Subramaniam, "18f-fdg pet/ct and melanoma: Value of fourth and subsequent posttherapy follow-up scans for patient management," *Clinical Nuclear Medicine*, vol. 41:9, pp. 403–409, 2016.

[26] F. van Leeuwen and M. de Jong, "Molecular imaging: the emerging role of optical imaging in nuclear medicine," *European Journal of Nuclear Medicine and Molecular Imaging*, vol. 41:11, pp. 2150–2153, 2014.

[27] N. I. of Biomedical Imaging and Bioengineering, "Optical imaging." `https://www.nibib.nih.gov/science-education/science-topics/optical-imaging`, 2016.

[28] V. Torchilin, "Liposomes as delivery agents for medical imaging," *Molecular Medicine Today*, vol. 2:6, pp. 242–249, 1996.

[29] F. G. Wouterlood and A. J. Boekel, "Fluorescence microscopy in the neurosciences," *Encyclopaedia of Neurosciences*, pp. 259–260, 2009.

[30] A. C. Croce and G. Bottiroli, "Autofluorescence spectroscopy and imaging: A tool for biomedical research and diagnosis," *European Journal of Histochemistry*, vol. 58:4, 2014.

[31] L. L. S. Solutions, "Cyanine dyes." `https://www.lumiprobe.com/tech/cyanine-dyes`, 2018.

[32] S. Srivastava, *Biomarkers in Cancer Screening and Early Detection*. Wiley Blackwell, 2017.

[33] M. Bradl, "Liposomes as drug carriers: a technological approach," *Biotechnology Annual Review*, vol. 7, pp. 59–85, 2001.

[34] L. Sercombe, T. Veerati, F. Moheimani, S. Wu, A. Sood, and S. Hua, "Advances and challenges of liposome assisted drug delivery," *Frontiers in Pharmacology*, vol. 6:286, 2015.

[35] S. Inamdar, R. Nitiyanandan, and K. Rege, "Emerging applications of exosomes in cancer therapeutics and diagnostics," *Biengineering & Translational Medicine*, vol. 2, pp. pages 70–80, 2017.

[36] K. M. ad K.L. Powell, A. Ashton, J. Morris, and S. McCracken, "Exosomes: Mechanisms of uptake," *Journal of Circulating Biomarkers*, vol. 4:7, 2015.

[37] L. G. Menona, V. J. Shi, and R. S. Carroll, *Mesenchymal stromal cells as a drug delivery system*. Harvard Stem Cell Institute Cambridge MA, 2009.

[38] S. Yao, X. Li, J. Liu, Y. Sun, and Z. Wang, "Maximized nanodrug-loaded mesenchymal stem cells by a dual drug-loaded mode for the systemic treatment of metastatic lung cancer," *Drug Delivery*, vol. 24:1, pp. 1372–1383, 2017.

[39] C. Rajagopal1 and K. B. Harikumar, "The origin and functions of exosomes in cancer," *Frontiers in Oncology*, vol. 8, 2018.

[40] M. Alférez, M. Barrionuevo, I. L. Aliaga, M. Sanz-Sampelayo, F. Lisbona, J. C. Robles, and M. Campos, "Digestive utilization of goat and cow milk fat in malabsorption syndrome," *Journal of Dairy Research*, vol. 68:3, pp. pages 451–461, 2001.

[41] R. Jennesl, "Composition and characteristics of goat milk: review," *Journal of Dairy Science*, vol. 63:10, pp. 1605–1630, 1980.

[42] Y. Nakamura, A. Mochida, P. L. Choyke, and H. Kobayashi, "Nanodrug delivery: Is the enhanced permeability and retention effect sufficient for curing cancer?," *Bioconjugate Chemistry*, vol. 27:10, pp. pages 2225–2238, 2016.

[43] S. Halvaei, S. Daryani, Z. Eslami-S, T. Samadi, N. Jafarbeik-Iravani, T. O. Bakhshayesh, K. Majidzadeh-A, and R. Esmaeili, "Exosomes in cancer liquid biopsy: A focus on breast cancer," *Molecular Therapy Nucleic Acids*, vol. 10, pp. 131–141, 2017.

[44] C. A. Franzen, P. E. Simms, A. F. V. Huis, K. E. Foreman, P. C. Kuo, and G. N. Gupta, "Characterization of uptake and internalization of exosomes by bladder cancer cells," *BioMed Research International*, vol. 2014, pp. 1–11, 2014.

[45] K. Vaswani, Y. Koh, F. Almughlliq, N. Peiris, and M. Mitchell, "A method for the isolation and enrichment of purified bovine milk exosomes," *Reproductive Biology*, vol. 17:4, pp. 341–348, 1980.

[46] H. Mohr and A. Völkl, "Ultracentrifugation," *Encyclopedia of Life Sciences*, 2017.

[47] S. Bio-Imaging, "Negative staining." `http://web.path.ox.ac.uk/~bioimaging/bitm/instructions_and_information/em/neg_stain.pdf`, 2004.

[48] V. Pospichalova, J. Svoboda, A. Kotrbova, K. Kaiser, D. Klemova, L. Ilkovics, A. Hampl, I. Crha, E. Jandakova, L. Minar, V. Weinberger, and V. Bryja, "Simplified protocol for flow cytometry analysis of fluorescently labeled exosomes and microvesicles using dedicated flow cytometer," *Journal of Extracellular Vesicles*, vol. 4, 2014.

[49] J. Schindelin, E. Frise, V. Kaynig, M. Longair, T. Pietzsch, S. Preibisch, C. Rueden, S. Saalfeld, B. Schmid, J.-Y. Tinevez, D. J. White, V. Hartenstein, K. Eliceiri, P. Tomancak, and A. Cardona, "Fiji: an open-source platform for biological-image analysis," *Nature Methods*, vol. 9:7, pp. 676–682, 2012.

[50] E. W. et al., "Cells release subpopulations of exosomes with distinct molecular and biological properties," *Nature Scientific Reports 6*, 2016.

[51] T. L. Riss, R. A. Moravec, A. L. Niles, S. Duellman, H. A. Benink, T. J. Worzella, and L. Minor, *Cell Viability Assays*. Sittampalam GS, Coussens NP, Brimacombe K, et al., editors, Betsheda, 2006.

[52] C. Thery, S. Amigorena, G. Raposo, and A. Clayton, "Isolation and characterization of exosomes from cell culture supernatants and biological fluids," *Current Protocols in Cell Biology*, vol. 3, 2006.

[53] S. S. e. I. Ministerio de Sanidad, "Informe anual del sistema nacional de salud, 2016." `https://www.msssi.gob.es/estadEstudios/estadisticas/sisInfSanSNS/tablasEstadisticas/InfAnSNS.htm`, 2016.

[54] W. B. van den Hout, "The value of productivity: human-capital versus friction-cost method," *Annals of Rheumatic Diseases*, vol. 69:1, pp. i89–91, 2010.

[55] F. Palencia-Sánchez and M. I. Riaño-Casallas, "Métodos de valoración de los costos indirectos de la enfermedad laboral," 2013.

[56] D. of Health, "Public awareness of cancer in britain: Report for the national awareness and early diagnosis initiative." `https://www.cancerresearchuk.org/`, 2009.

[57] C. Petrini, "Ethical and legal considerations regarding the ownership and commercial use of human biological materials and their derivatives," *Journal of Blood Medicine*, vol. 3, pp. 87–96, 2012.